

# Petrological and geochemical (trace elements and Sr–Nd isotopes) characteristics of the Paleozoic Kovdor ultramafic, alkaline and carbonatite intrusion (Kola Peninsula, NW Russia)

A. Verhulst <sup>a</sup>, E. Balaganskaya <sup>b</sup>, Y. Kirnarsky <sup>b</sup>, D. Demaiffe <sup>a,\*</sup>

<sup>a</sup> *Géochimie Isotopique, CP 160 / 02, Univ. Libre de Bruxelles, 50 Av. Roosevelt, 1050 Brussels, Belgium*

<sup>b</sup> *Geological Institute, Kola Scientific Centre, 14 Fersman Street, 184200 Apatity, Russian Federation*

Received 15 January 1999; accepted 12 July 1999

## Abstract

The Kovdor intrusion belongs to the Paleozoic (380–360 Ma) Kola alkaline and carbonatite province (NW Russia). It displays a complete sequence of rocks that include in order of intrusion, ultramafic rocks, melilitolites, alkaline silicate rocks of the melteigite–ijolite series, phoscorites and carbonatites, and late nepheline syenite dykes (the latter were not studied). The ultramafic sequence (dunite–peridotite–clinopyroxenite) consists of olivine–clinopyroxene cumulates (Mg# = 86–70) with intercumulus phlogopite and magnetite and late calcite. Melilitolites, with up to 35 wt.% CaO (melilite cumulates), have a magmatic rather than metasomatic origin. Rocks of the melteigite–ijolite series are very heterogeneous (variations of grain size, mineralogy and modal proportions) and show disequilibrium textures (core resorption and complex zoning of the clinopyroxenes) suggesting either magma mixing or contamination. All the rocks have strong incompatible element enrichments in multi-element spidergrams. The rare earth element (REE) patterns are steep with  $(La/Yb)_N > 20$ ; they are subparallel and do not show any Eu anomaly. The variations of Nb/Ta ratios and the REE distributions suggest that the carbonatites and the rocks of the melteigite–ijolite series are not conjugate immiscible liquids. Most rocks (ultramafics, melilitolites, carbonatites and phoscorites) plot in the depleted mantle quadrant of the Nd–Sr diagram with low  $(^{87}Sr/^{86}Sr)_i$  ratios (0.70332 to 0.70377) and positive  $\varepsilon_{Nd}(t)$  values (+5.2 to +0.6). The fairly large range of isotopic compositions is not in favour of a simple, closed system magmatic evolution; it suggests a complex evolution implying several magma batches derived either from an isotopically heterogeneous mantle source or from various mixing proportions of two mantle reservoirs. The isotopic composition of the melteigites–ijolites requires a slightly enriched component that could be similar to that of the Kandalaksha ultramafic lamprophyres and of the Tersky Coast and Arkhangelsk kimberlites. © 2000 Elsevier Science B.V. All rights reserved.

**Keywords:** Carbonatites; Alkaline complexes; Kola Peninsula; Melilitolites; Ultramafic rocks

\* Corresponding author. Tel.: +32-2-6503686; fax: +32-2-6502226; e-mail: ddemaif@ulb.ac.be

## 1. Introduction

Carbonatites are rare, mantle-derived magmatic rocks mainly found in stable, intraplate continental settings (Heinrich, 1966; Bell, 1989). They are commonly related to major lineaments (rifts) or to doming, and often form provinces of clustered intrusions, i.e., in East Africa (Le Bas, 1977; Bell and Blenkinsop, 1987a), S. Brazil (Morbidelli et al., 1995), Greenland (Nielsen, 1980; Larsen and Rex, 1992), E. Canadian shield (Bell and Blenkinsop, 1987b), and Kola Peninsula, Russia (Kogarko et al., 1995). Plutonic carbonatites are commonly associated with a large range of alkaline silicate rocks, including ultramafic rocks, turjaites–melilitolites, ijolites–melteigites and nepheline syenites.

This paper focuses on the Kovdor massif, a complex intrusion belonging to the Paleozoic Kola alkaline and carbonatitic province (Kukhareno et al., 1965; Kogarko, 1987; Kogarko et al., 1995; Kramm et al., 1993; Arzamastsev, 1994). The Kovdor massif is an illustrative intrusion of the Kola province as it displays a large sequence of rocks including olivine- and clinopyroxene-rich ultramafic rocks, melilitolites, various alkaline silicate rocks and several generations of carbonatites and phoscorites. It is one of the most well-known complexes of this province as outcrops are common and mining operations (for magnetite and phlogopite) have excavated huge quarries.

We present new petrological, mineralogical and geochemical data (major and trace elements, Sr and Nd isotopes) on the main rock types, in order to describe the magmatic processes and to constrain the genetic relations between the carbonatites, the ultramafic rocks and the alkaline silicate rocks of the Kovdor intrusion.

## 2. Geological setting

The Kola Peninsula forms the northeastern part of the Baltic Shield and is mainly composed of three Archean to Proterozoic (2.9–1.7 Ga) crustal terranes (Kratz et al., 1978; Mitrofanov, 1995). During the Paleozoic, numerous ultramafic, alkaline and carbonatitic intrusions were emplaced over an area of more

than 100 000 km<sup>2</sup> which extends from eastern Finland to eastern Kola Peninsula (Fig. 1a). Two major structural lineaments appear to control the emplacement of the alkaline complexes of the Kola Alkaline Province: the Kontozero graben and the Kandalaksha deep fracture zone, which are, respectively, perpendicular and parallel to the NW–SE trending Proterozoic structure of the Kola Peninsula (Dudkin and Mitrofanov, 1994). Mineral Rb–Sr age determinations on seven complexes of the Kola alkaline province have yielded a narrow range of 380–360 Ma (Kramm et al., 1993), corresponding to latest Middle Devonian to Upper Devonian.

The Kovdor massif (Fig. 1b) (40 km<sup>2</sup>) is a complex, multiphase, concentric intrusion (Kukhareno et al., 1965; Kogarko et al., 1995). It intrudes Archean biotite–gneisses and granitic gneisses of the Belomorian group. Emplacement of the Kovdor complex was controlled by the Kandalaksha deep fault zone (Kogarko et al., 1995; Bell et al., 1996). The contacts are subvertical and gravimetric data show that the massif extends down to 12 km (Arzamastsev et al., 1996). A U–Pb age determination on baddeleyite (from carbonatite) yielded an age of  $380 \pm 4$  Ma (Bayanova et al., 1997). The general geology of Kovdor has been extensively described by Kukhareno et al. (1965) and more recently summarised and updated by Arzamastsev (1994; 1995) who suggested that the melilitolites–turjaites intruded before the alkaline silicate rocks. The main rock types are, from the oldest to the youngest, ultramafic rocks (dunite and clinopyroxenite), turjaites and melilitolites, rocks of the ijolite–melteigite series, apatite–forsterite–magnetite rocks (phoscorite) of the ore complex, carbonatites and nepheline syenites. In fact, melilite-bearing melteigite could belong to the melilitolite series and not to the ijolite–melteigite series (see below).

Ultramafic rocks constitute a huge central zone with a dunite (= olivinite) core rimmed by two semi-annular intrusions of peridotite (= diopside olivinite) to the north and of clinopyroxenite to the south. The olivine-rich rocks have been termed olivinite by the Russian authors because they contain magnetite instead of chromite, indicating that they crystallized from a somewhat evolved, Cr-poor melt. Turjaite, monticellite–melilite rocks and melilitolite form irregular bodies between the ultramafic core

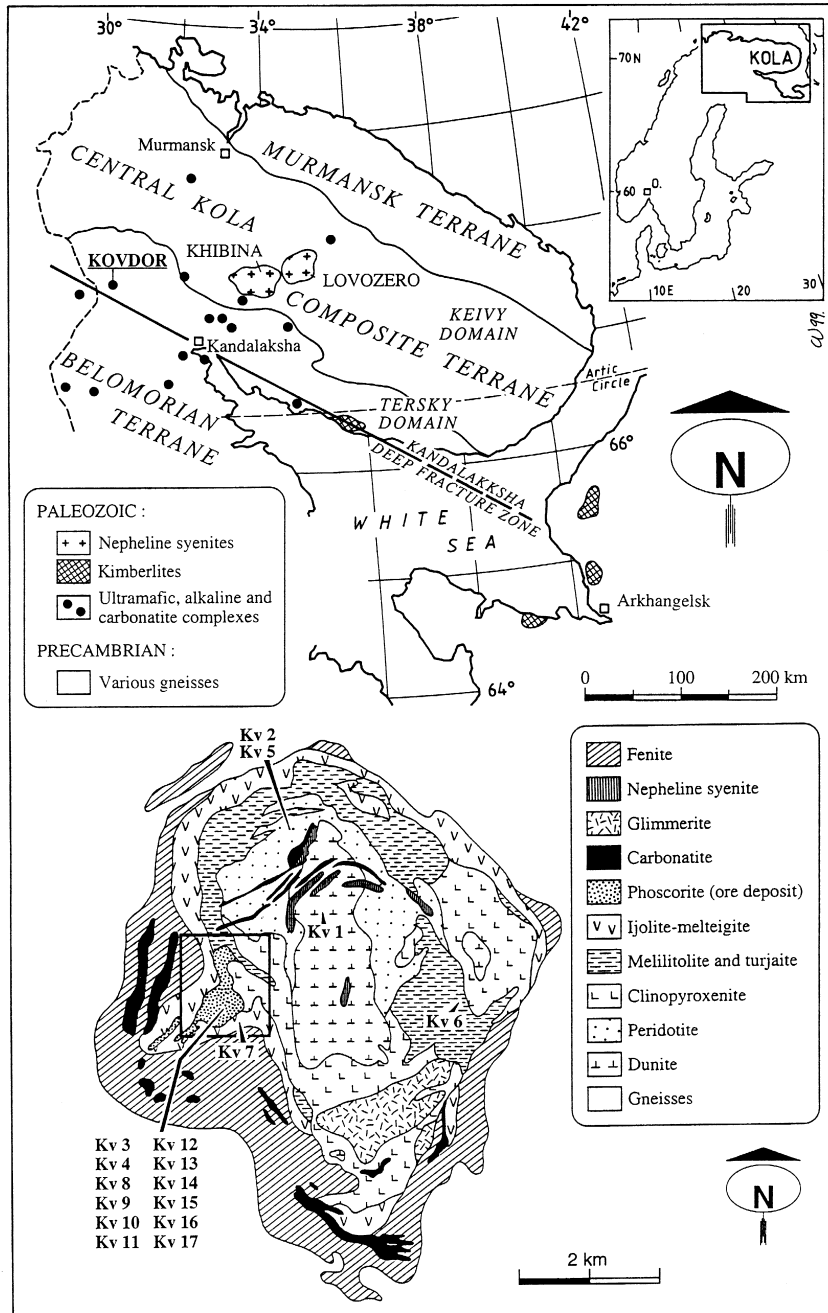


Fig. 1. (a) Overview map of the Kola Peninsula showing the Precambrian terranes and the Paleozoic alkaline and carbonatite intrusions (from Balagansky and Glaznev in Gee and Zeyen, 1996). (b) Sketch map of the Kovdor intrusion (from Ternovoy et al., 1969) with sample locations.

Table 1

Mineralogical composition of the Kovdor rocks

+++ : &gt; 30 vol.%, ++ : 10–30 vol.%, + : 5–10 vol.%, + : &lt; 5 vol.%.

DUN: dunite; PRD: peridotite; PRX: clinopyroxenite; MLT: melilitolite; Me-MLG: melilite-bearing melteigite; MLG: melteigite; IJL: ijolite; Ph: phoscorite; C I: calcite carbonatite of the first stage; C II: calcite carbonatite of the second stage; C III: dolomite carbonatite.

Sample identification	Kv1	Kv2	Kv3	Kv4	Kv5	Kv6	Kv7	Kv8	Kv9	Kv10	Kv11	Kv12	Kv13	Kv14	Kv15	Kv16	Kv17
Rock type	Ko562-56	Ko22B	Ko21	Ko864-83	Ko22A	Ko54	Ko63	Ko16A	Ko57	Ko864-33	Ko17A	Ko15A	Ko15B	Ko15C	Ko20A	Ko18	Ko20C
	DUN	DUN	PRD	PRX	MLT	MLT	Me-MLG	MLG	MLG	IJL	Ph	C I	C I	C II	C III	C III	C III
Olivine	+++	+++	+++								++	+	+		+		
Diopside	+	+	++	+++	+	+	+++		++								
Aegirine–augite								+++	+++	++							
Melilite					+++	+++	+										
Nepheline						+	++	++	++	+++							
Alkali feldspar										+							
Phlogopite	+	+	++	++	+	+					+++	+	+	+			
Tetraferri-phlogopite		+	+										+		++	+	+
Biotite								+	+	+							
Magnetite	+	+	++	+	+	+	+	+	+		++	++	++	++	++	+	+
Sulfides								+								+	+
Calcite	+		+	+		+		+	+		+	+++	+++	+++	+++	+	+
Dolomite											+	+	+	+	+	+++	+++
Apatite		+						+	+	+	+	+	+	+	+	+	+
Perovskite				+			+	+								+	+
Andradite				+	+	+											
Scholormite							+										
Titanite								+	+								
Monticellite					+	+											
Wollastonite					+												
Pyrochlore															+	+	+
Baddeleyite														+	+		
Clinohumite	+	+									+				+		
Cancrinite						+		+	+								
Vesuvianite						+											
Cebollite (?)						+											
Zeolite								+	+								

and the external intrusion which is mainly composed of rocks of the ijolite–melteigite series.

The phoscorite–carbonatite ore complex (0.8 × 1.3 km) intrudes the clinopyroxenites and the ijolites–melteigites in the southwestern part of the massif. It is currently mined for magnetite and apatite (with subsidiary Cu-sulphides and baddeleyite concentrates). The complex consists of several generations of magnetite rich-ores and apatite–forsterite rich-rocks (phoscorites) associated with carbonatites (Krasnova and Kopylova, 1988). The phoscorites form subvertical pipe-like bodies and the carbonatites form a steep-dipping stockwork of veins. Calcite carbonatite and dolomite carbonatite are both present in the ore complex: the former constitutes irregular bodies (100–500 m in diameter) while the latter forms numerous 0.7–1 m wide veins (Kukharensko et al., 1965). Late stage nepheline syenite occurs as veins or dykes in the central part of the massif. Intrusion of the Kovdor complex caused fenitization of the surrounding country rocks. The fenite zone is semi-annular, widening from the north to southwest (300–350 m up to 4 km wide).

The list of analyzed samples with a brief petrographic description and mineralogical composition is given in Table 1.

In this paper, we follow the IUGS recommendations for the classification of igneous rocks (Le Maitre, 1989), the nomenclature of carbonatites proposed by Woolley and Kempe (1989) and Woolley et al. (1996) and the recent classification scheme for melilitolites given by Dunworth and Bell (1998). The local names, provided for some rocks by the Russian scientists who have studied the Kola alkaline province in detail, are mentioned between brackets. The term phoscorite was defined for the first time by Russel et al. (1954) at Phalaborwa (South Africa).

### 3. Petrographic description and mineral chemistry

The samples selected for geochemical investigations are briefly described below. Selected electron microprobe data of the main minerals (olivine, clinopyroxene, melilite and phlogopite) are listed in Table 2. Microprobe analyses were performed on a Cameca Camebax SX 50 wavelength-dispersive mi-

croprobe at the ‘Centre d’Analyses par Microsonde pour les Sciences de la Terre (CAMST)’ (University of Louvain-la-Neuve, Belgium). The operating conditions were: accelerating voltage 15 kV, beam current 20 nA and a PAP matrix correction program (Pouchou and Pichoir, 1991). Standards used were a combination of natural and synthetic minerals.

*Dunites* (Kv1 and Kv2) are medium- to coarse-grained rocks essentially composed (> 90 vol.%) of subhedral to anhedral olivine (Fo<sub>86–90</sub>; 0.2–0.3 wt.% NiO; Cr content is below detection limit, < 0.1% Cr<sub>2</sub>O<sub>3</sub>) with variable amounts of interstitial magnetite, phlogopite, apatite and calcite (Fig. 2a). Diopside (Wo<sub>51</sub>En<sub>43</sub>Fs<sub>6</sub>) is rare (one or two grains per thin section). Some dunites (Fig. 2b) are locally enriched in phlogopite, magnetite and/or apatite (Kukharensko et al., 1965). The dunites are clearly olivine cumulates and display textures close to adcumulates. The olivine cores contain orientated lamellar and/or bleb-like inclusions that consist of intimately intergrown diopside and magnetite that form a symplectitic association. Diopside and magnetite were possibly exsolved from a primary olivine that contained Fe<sup>3+</sup> ions (Moseley, 1984). The exsolution hypothesis is supported by the differences in chemical compositions between the diopside included in the olivines and the interstitial grains between olivine crystals. The interstitial diopside has measurable Al<sub>2</sub>O<sub>3</sub> and TiO<sub>2</sub> contents (1.24 and 0.5 wt.%, respectively), lower SiO<sub>2</sub> content (~ 53 wt.%) and Mg number [Mg# = 88.2, with Mg# = 100 \* Mg / (Mg + Fe<sup>2+</sup>) in atomic proportions]. The exsolved diopside has no detectable Al<sub>2</sub>O<sub>3</sub> and TiO<sub>2</sub>, higher SiO<sub>2</sub> (~ 55 wt.%) and Mg# (~ 94). Interstitial magnetite has variable Cr<sub>2</sub>O<sub>3</sub> content: Bykova and Iljinsky (1978) have reported values as high as 6 wt.% but in the dunites studied in this paper, Cr is below detection limit. Phlogopite is often zoned: a green core (Mg# = 88–89) is surrounded by a thin rim of tetraferriphlogopite (Mg# = 83). This mica contains 0.93 wt.% BaO and 0.2 wt.% Cr<sub>2</sub>O<sub>3</sub> (in the core) which favours a magmatic rather than a metasomatic origin.

*Peridotites* are coarse-grained cumulate rocks with various modal proportions of olivine (Fo<sub>88</sub>; 0.1–0.2 wt.% NiO; Cr<sub>2</sub>O<sub>3</sub> generally below detection limit, but locally up to 0.2 wt.%) and intercumulus diopside, Ti-magnetite and green phlogopite. The olivines



Table 2 (continued)

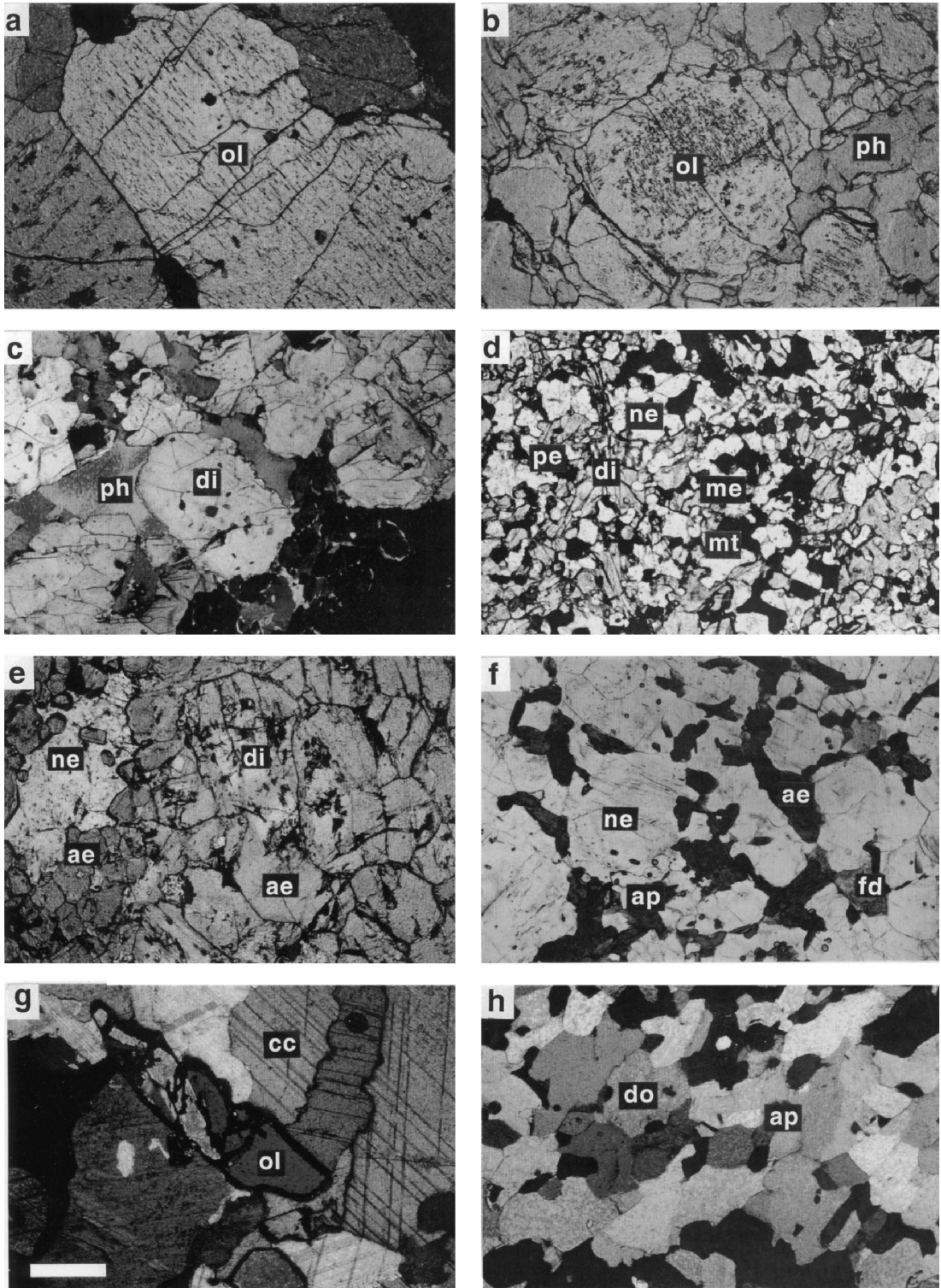
Sample Rock type	Phlogopite/biotite										
	Kv1	Kv3	Kv3	Kv4	Kv5	Kv8	Kv11	Kv13	Kv13	Kv15	Kv17
	DUN core ph	PRD core ph	PRD rim ph	PRX core ph	MLT core ph	MLG core bi	Ph core ph	C I core ph	C I rim ph	C II core ph	C III core ph
SiO <sub>2</sub>	38.24	41.22	42.47	37.93	39.93	37.70	35.63	41.44	42.15	42.31	41.46
TiO <sub>2</sub>	0.61	0.64	0.86	1.62	0.09	2.60	0.57	0.41	0.09	0.14	–
Al <sub>2</sub> O <sub>3</sub>	16.31	12.31	9.75	14.21	14.80	11.56	19.31	12.02	6.29	9.43	7.39
Cr <sub>2</sub> O <sub>3</sub>	0.25	0.08	0.14	–	0.14	–	–	0.08	–	–	–
FeO	5.76	4.02	5.57	8.05	3.70	17.44	2.54	4.51	9.98	5.07	8.12
MnO	–	0.07	0.16	0.16	0.06	0.32	–	–	–	0.08	–
MgO	23.73	25.07	25.38	21.94	24.07	14.29	22.99	26.01	26.16	25.67	26.73
CaO	–	–	–	–	0.09	–	–	–	0.10	–	–
BaO	0.93	n.a.	n.a.	n.a.	n.a.	n.a.	n.a.	n.a.	n.a.	n.a.	n.a.
Na <sub>2</sub> O	0.79	0.78	0.81	1.33	1.00	0.17	1.25	0.66	0.66	0.22	1.30
K <sub>2</sub> O	9.22	9.84	10.20	8.53	9.35	10.50	8.02	10.08	10.07	11.33	9.06
NiO	–	n.a.	n.a.	n.a.	n.a.	n.a.	n.a.	n.a.	n.a.	n.a.	n.a.
F	n.a.	n.a.	n.a.	0.27	–	–	–	–	–	–	0.39
Cl	n.a.	n.a.	n.a.	–	–	–	–	–	–	–	–
H <sub>2</sub> O calc.	4.19	4.17	4.18	3.95	4.15	3.89	4.06	4.23	4.11	4.20	3.90
.-O=F	–	–	–	–0.11	–	–	–	–	–	–	–0.16
.-O=Cl	–	–	–	–	–	–	–	–	–	–	–
Total	100.03	98.20	99.52	97.88	97.29	98.47	94.37	99.44	99.51	98.45	98.19
Mg#	88	92	89	83	92	59	94	91	82	90	85

also show numerous symplectitic inclusions of magnetite and diopside and contain grains of magnetite. Sample Kv3, collected near the ore complex (phoscorite), shows greenish material filling the cracks of the olivine grains or surrounding these grains. Cathodoluminescence (CL) studies indicate that most of the veinlets are composed of calcite (Verhulst et al., 1997). The clinopyroxene is a Ti- and Al-rich diopside ( $Wo_{51-52}En_{41-44.5}Fs_{4.5-7}$  with 1.4–3.5 wt.% Al<sub>2</sub>O<sub>3</sub> and 0.5–0.8 wt.% TiO<sub>2</sub>); it is complexly zoned with an overgrowth of Al- and Ti-poor diopside. The Na content is always low (< 0.3 wt.% Na<sub>2</sub>O). Interstitial Ti–magnetite (1.6–5.2 wt.% TiO<sub>2</sub>, 1.4–2.2 wt.% MgO, 0.5–0.8 wt.% MnO) has Cr<sub>2</sub>O<sub>3</sub> content between 1.0 and 1.4 wt.%. Phlogopite (Mg# = 89) forms large euhedral to subhedral poikilitic grains that tend to enclose and/or replace the diopside. A thin rim of tetraferriphlogopite mantles the green mica. Calcite fills the interstices.

*Clinopyroxenites* (Kv4) are coarse-grained rocks composed of > 85 vol.% subhedral to anhedral, partly resorbed, diopside (~  $Wo_{50}En_{45}Fs_5$ , with < 0.3 wt.% Na<sub>2</sub>O). Ti–magnetite, green phlogopite

and calcite crystallized in the interstices; large phlogopite (Mg# = 83) grains fill the diopside embayments (Fig. 2c). The clinopyroxenite is probably an ortho- to meso-cumulate, although the cumulate texture was largely obliterated by the replacement of clinopyroxene by mica giving rise to interpenetrated association. Magnetite crystallized before phlogopite. Secondary perovskite (mantling magnetite) and melanite (4.7–13.5 wt.% TiO<sub>2</sub>) are common. Calcite is the latest phase, filling the interstices or crystallizing as small grains along grain boundaries.

*Melilite-rich rocks* constitute a very heterogeneous group that includes turjaite, ultramelilitolites and monticellite (± garnet)-bearing varieties. They differ in their modal mineralogy and texture (Kukharenko et al., 1965). Turjaite is the main rock type; it is composed of melilite (25–50 vol.%), nepheline (15–30 vol.%), phlogopite (20–25 vol.%) and diopside (5–25 vol.%) (Arzamastsev, 1994). The ultramelilitolite (> 85 vol.% melilite and < 5 vol.% nepheline) forms lenticular bodies in turjaite. Monticellite melilitolite constitutes irregular zones in the ultramafic rocks. The heterogeneous nature of these



rocks and the presence of skeletal olivine surrounded by an aggregate of monticellite and diopside (itself replaced by andradite) were arguments in favour of a metasomatic origin (Kukhareenko et al., 1965). A more recent study of glass inclusions in melilite, however, supports a magmatic origin for turjaite (Sokolov, 1989).

The samples studied are coarse-grained *ultra-melilitolites*, composed of > 85 vol.% anhedral melilite. The melilite grains are slightly intergrown with irregular outlines, suggesting an adcumulate texture. Sample Kv5 was collected in the phlogopite quarry. The average composition of the melilite ( $\text{SM}_{18.5-25}\text{Ge}_{0.7-3.7}\text{Åk}_{71.5-80.5}$ ; Åk includes Fe-Åk) is typical of igneous melilites (Mitchell, 1996). Melilite is poikilitic with numerous orientated inclusions of wollastonite and monticellite. These two minerals are the products of the subsolidus destabilisation of the åkermanite (Harker and Tuttle, 1956; Mitchell, 1996). In sample Kv6 (collected in the melilitolite–turjaite intrusion, in the southwestern part of the complex), melilite appears locally transformed to an assemblage of vesuvianite, calcite and a fibrous mineral (cebolite?). The relative development of these secondary minerals varies widely from grain to grain. Green phlogopite, nepheline, cancrinite, Ti–magnetite and relics of diopside ( $\sim \text{Wo}_{50}\text{En}_{45}\text{Fs}_5$ , with < 0.2 wt.%  $\text{Na}_2\text{O}$ ) are common accessory minerals. Subsidiary reactions typically form zoned andradite (brown Ti-rich core and pale yellow Ti-rich rim; e.g., Platt, 1996) around the magnetite. In sample Kv6, large pyroxenes are partly resorbed and mantled by aggregates of monticellite, mica and scholormite. Large zoned phlogopites are corroded and replaced by a mosaic of small cancrinite, nepheline, natrolite (?) and andradite.

The *ijolite–melteigite series* rocks are also very heterogeneous in terms of texture, grain size and

mineralogy. Sample Kv7 is a fine- to medium-grained, layered cumulate rock, composed of subhedral to anhedral diopside ( $\text{Wo}_{49-50}\text{En}_{42}\text{Fs}_{8-9}$ , with up to 0.6 wt.%  $\text{Na}_2\text{O}$ ), melilite ( $\text{SM}_{41-46}\text{Ge}_{0.4-1.4}\text{Åk}_{54-59}$ ), perovskite and interstitial nepheline ( $\text{Qz}_0\text{Ne}_{79.5-81}\text{Ks}_{19-21.5}$ ), and Ti–magnetite (5.5 wt.%  $\text{TiO}_2$ , 1.3 wt.%  $\text{Al}_2\text{O}_3$ , 1.0 wt.%  $\text{MnO}$ ) (Fig. 2d). Similar Na-rich melilite has been reported for a turjaite from the Turiy Mys complex (Bell et al., 1996). Scholormite (15.5 wt.%  $\text{TiO}_2$ ) is accessory. Partly resorbed clinopyroxenes contain abundant fluid and glass inclusions and enclose small inclusions of nepheline. Ti–magnetite and nepheline are interstitial. On the basis of its modal mineralogy (dominant clinopyroxene and nepheline), this sample is a melteigite but, in contrast to the other ijolites–melteigites, it contains melilite that is not a characteristic mineral in that series. In that sense, Kv7 is probably better described as a nepheline–pyroxene-rich melilitolite rather than as a melteigite. This sample also has distinct geochemical and isotopic features (see below). Two melteigites (Kv8 and Kv9) were collected in the top of the wall of the iron deposit. They are fine- to medium-grained rocks composed of aggregates of clinopyroxene (diopside to aegirine–augite:  $\text{Wo}_{49}\text{En}_{47}\text{Fs}_4$  to  $\text{Wo}_{43}\text{En}_{29}\text{Fs}_{28}$ , with 0.4–3.2 wt.%  $\text{Na}_2\text{O}$ ) and interstitial nepheline ( $\text{Qz}_{9.5-10.5}\text{Ne}_{68.5}\text{Ks}_{20.5-21.5}$ ) with minor magnetite, biotite and apatite. Titanite is rather abundant (5–10 vol.%). Clinopyroxene and titanite are either euhedral (sample Kv9) or anhedral (sample Kv8). Biotite and calcite partially replace clinopyroxene. Disequilibrium textures are observed in sample Kv9: the size of the clinopyroxene grains is highly variable (< 0.1–3 mm) and the grains are complexly zoned with a resorbed core of aegirine–augite (less frequently diopside) surrounded by several overgrowths of aegirine–augite alternating with diopside (Fig. 2e). In

Fig. 2. (a) Coarse-grained dunite (Kv1) showing large subhedral olivine (*ol*) with numerous diopside–magnetite inclusions (see text). (b) Medium-grained dunite (Kv2) with interstitial (= intercumulus) phlogopite (*ph*). Note the melt inclusions in the olivine. (c) Medium-grained clinopyroxenite (Kv4) with euhedral diopside (*di*) and interstitial phlogopite. (d) Fine- to medium-grained melilite (*me*)-bearing melteigite (Kv7) with diopside, interstitial nepheline (*ne*), magnetite (*mt*) and perovskite (*pe*). (e) Heterogeneous melteigite (Kv9). Note the variable grain size of the cpx. Large cpx show complex zoning texture with relict diopside (*di*) core and aegirine–augite (*ae*) broad rim. Small cpx are aegirine–augite. (f) Ijolite (Kv10) with euhedral to subhedral nepheline (*ne*) and interstitial aegirine–augite (*ae*), apatite (*ap*) and slightly altered alkali feldspar (*fd*). (g) Coarse-grained olivine (*ol*)-bearing calcite carbonatite of the first stage (Kv14). (h) Fine-grained dolomite (*do*) carbonatite (Kv17) with small apatite (*ap*) grains. All photomicrographs at the same scale, the bar corresponds to 0.5 mm.

sample Kv8, a few grains of perovskite are present, included in titanite. The latter also forms large aggregates between resorbed aegirine–augite crystals. Apatite is accessory and crystallized before nepheline in the interstices between the clustered clinopyroxenes. Nepheline is partially replaced by cancrinite and zeolites are developed in the interstices, especially in sample Kv9. Sample Kv10 (from a drill-core) is a fine-grained ijolite composed of nepheline (locally replaced by minor cancrinite) and clinopyroxene with minor, slightly altered, alkali feldspar and apatite. This ijolite is transitional to urtite in view of its high modal proportion of subhedral nepheline (Fig. 2f).

Six stages of *phoscorite* (Ia, Ib, IIa, IIb, IIIa and IIIb) emplacement have been described by Krasnova and Kopylova (1988); carbonatite veins are associated with the last four phoscorite stages. Locally, the phoscorites have a brecciated texture with numerous blocks (or enclaves) of ultramafic rocks, ijolite, phoscorite or carbonatite. Xenocrysts of Fe-rich chromite, mantled by magnetite have been identified together with rounded fragments of dunite and phoscorite in the explosive breccia of the second stage (IIb) (Balaganskaya, 1994). These rocks are very heterogeneous, they have not been sampled systematically. Phoscorites are mined for magnetite that occurs as millimeter to centimeter size euhedral to anhedral grains. The studied sample (Kv11) belongs to stage Ia. These fine-grained phoscorites are composed of forsterite, green phlogopite, Ti–magnetite, clinohumite, apatite and calcite. Olivine ( $\text{Fo}_{93-95}$ ) appears as small (0.15–0.35 mm) inclusion-rich rounded grains. Small anhedral magnetites are irregularly distributed between the silicates, they locally form lenticular zones of interstitial Ti–magnetite (4.3 wt.%  $\text{TiO}_2$ , 0.9%  $\text{Al}_2\text{O}_3$ , 5.4 wt.% MgO and < 0.1 wt.%  $\text{Cr}_2\text{O}_3$ ). Clinohumite appears as poikilitic crystals. Sample Kv11 shows a flow texture with grain size variations and olivine- or apatite-rich layers. Several generations of phlogopite are observed: large phlogopite flakes, lath-shaped subhedral grains between the olivine, clinohumite and phlogopite and anhedral interstitial mica.

The Kovdor *carbonatites* are calcite carbonatites, with diopside-bearing and forsterite-bearing varieties, and late-stage dolomite carbonatites. Two stages of calcite carbonatites were identified in the field (Krasnova and Kopylova, 1988); they are also

distinguishable by their mica compositions: green phlogopite in the first stage and red tetraferriphlogopite in the second stage.

*Calcite carbonatites* are medium- to coarse-grained, sometimes gently flow-banded cumulate rocks, essentially composed of anhedral calcite with variable amounts of apatite, green or red phlogopite, magnetite, and forsterite, locally forming discontinuous layers. Baddeleyite, uranpyrochlore (exclusively in the second stage) and dolomite are the main accessory minerals. Coarse calcite (commonly twinned) grains are highly interlocked giving a consertal texture (McKenzie et al., 1987). Forsterite ( $\text{Fo}_{91.8-93.7}$ ) is an early crystallization phase, partially corroded and slightly serpentinized or replaced by clinohumite (Fig. 2g). Symplectitic inclusions of diopside and magnetite are not observed in the olivines. Apatites are subhedral stubby rounded grains of variable size. Euhedral to subhedral phlogopite is sometimes rimmed by tetraferriphlogopite and shows frequent embayments. Apatite and phlogopite are often located along calcite grain boundaries. Ti–magnetite forms small aggregates surrounded by thin flakes of mica or large euhedral crystals (calcite carbonatite of the second stage).

*Dolomite carbonatites* occur as veins (< 1 m wide) crosscutting the calcite carbonatites of the two stages (Krasnova and Kopylova, 1988). Two stages of dolomite carbonatite follow the last two stages of phoscorite. The studied samples (Kv16 and Kv17) are fine-grained rocks composed of dolomite with minor calcite, apatite and tetraferriphlogopite (Fig. 2h). Accessory minerals are uranpyrochlore, pyrrhotite, magnetite and ilmenite. Anhedral grains of dolomite (untwinned) show straight boundaries and frequent triple-junction points. Calcite is interstitial. Micas are partially corroded and replaced by chlorite or calcite along cleavages. A metamict rim is developed around the small grains of uranpyrochlore in the dolomite crystals.

#### 4. Analytical methods

Each sample selected for bulk rock major and trace elements and isotopic analysis has been carefully crushed and grinded in a stainless steel mortar. The major elements of the silicate rocks were anal-

ysed either by X-ray fluorescence (XRF) spectrometry using the borate fusion technique (except for sodium which was measured on a pressed powder pellet) at the ‘Collectif de Géochimie instrumentale’ (University of Liège) (samples Kv2, Kv3, Kv4 and Kv5) or by inductively coupled plasma (ICP) emission spectrometry at the SARM (Service d’Analyses des Roches et des Minéraux) of the CRPG, Nancy (samples Kv1, Kv6, Kv7, Kv8, Kv9 and Kv10). The data include loss of ignition in the total. The carbonatites were measured by ICP and their CO<sub>2</sub> contents were determined by the coulometry technique. The FeO content of carbonatites and silicate rocks was done by K<sub>2</sub>Cr<sub>2</sub>O<sub>7</sub> titration at the ‘Département des Sciences de la Terre’, University of Brussels (Belgium). Trace element abundances (including the rare earth elements, REE) were measured by inductively coupled plasma emission mass spectrometry (ICP-MS) at the ‘Département de géologie du Musée Royal de l’Afrique Centrale’ in Tervuren (André and Ashchepkov, 1996). The precision of the major element analyses is better than 2% for XRF and ICP in most cases, but in the range 2–10% for low content elements (< 0.5%). The precision of the trace elements analyses is < 5% for content above 1 ppm and between 10 and 15% for the 0.1–1 ppm range (Navez, 1995).

Rb and Sr concentrations were determined by XRF using pressed powder pellets at the University of Brussels (ULB). Nd and Sm contents were obtained either by ICP-MS or by isotope dilution mass spectrometry. Samples were dissolved in a mixture of HF–HClO<sub>4</sub> (10:1) or in a mixture of HF–HNO<sub>3</sub> (10:1). Chemical separation of Rb, Sr, Sm and Nd was carried out by cation-extraction chromatography on columns. Laboratory blank values for the whole procedure were < 1 ng for each of the elements analyzed. The Sr and Nd isotopic compositions were measured on a VG Sector 54 multicollector thermal ionization mass spectrometer. Isotope dilution analyses were carried out on a MAT 260 single collector mass spectrometer. Systematic measurements of the NBS 987 Sr standard during this study gave an average <sup>87</sup>Sr/<sup>86</sup>Sr value of 0.710267 ± 0.000007 (normalized to <sup>86</sup>Sr/<sup>88</sup>Sr = 0.1194). The MERCK Nd standard gave an average <sup>143</sup>Nd/<sup>144</sup>Nd value of 0.512742 ± 0.000008 (normalized to <sup>146</sup>Nd/<sup>144</sup>Nd = 0.7219). The measured isotopic compositions were

not corrected for these standard biases. The initial Sr and Nd isotopic ratios were calculated at 380 Ma using the decay constants of 1.42 × 10<sup>-11</sup> a<sup>-1</sup> (<sup>87</sup>Rb) and 6.54 × 10<sup>-12</sup> a<sup>-1</sup> (<sup>147</sup>Sm) (Steiger and Jäger, 1977).

## 5. Results

### 5.1. Major and trace element geochemistry

The major and trace elements contents of the carbonatites and related silicate rocks of the Kovdor massif are given in Tables 3 and 4.

Major elements variations are shown in Harker diagrams (oxides vs. MgO content) and compared to the data of Arzamastsev (1994) (Fig. 3). The MgO content shows a quite large variation in the ultramafic rocks, decreasing from 45.8 to 17 wt.% (Mg# = 86–70) according to the emplacement sequence, i.e., from dunite–peridotite to clinopyroxenite. With decreasing MgO content, there is an increase in SiO<sub>2</sub>, TiO<sub>2</sub>, Al<sub>2</sub>O<sub>3</sub>, FeO<sub>tot</sub>, CaO and K<sub>2</sub>O contents. The Na<sub>2</sub>O, MnO and P<sub>2</sub>O<sub>5</sub> contents are low. The observed chemical variations are within the range of those of Arzamastsev (1994), although his data appear more scattered. The compositional variation reflects the proportions of the liquidus phases and the various amounts of intercumulus material (mainly represented by phlogopite and magnetite) in the ultramafic cumulates.

The two analysed ultramelilitolites also have a high Mg# (79–80) with moderate MgO (9.3–10.8 wt.%) but exceptionally high CaO content (30.2–34.6 wt.%) that could indicate a cumulative origin (melilitite accumulation). By contrast, the CaO content is significantly lower (< 27 wt.%) in the samples analyzed by Arzamastsev that correspond to turjaites rather than to melilitolite.

The rocks of the ijolite–melteigite series are typically silica-undersaturated (39.4–45.4 wt.%), more differentiated (Mg# = 69–39) and alkali-rich (up to 13 wt.% Na<sub>2</sub>O and 3.5 wt.% K<sub>2</sub>O) with agpaitic index (A.I. = (Na + K)/Al) varying from 0.99 to 1.43. Melteigite Kv9 has an unusual composition: it has the highest Mg# and also a high A.I.

The phoscorites have not been systematically analysed because of their very heterogeneous nature

Table 3

Major and trace element composition of the silicate rocks and the carbonatites from Kovdor

Major elements in wt.%; trace elements in ppm.

1: analyzed by XRF spectrometry; 2: analyzed by ICP emission spectrometry.

n.a. = not analyzed.

Sample	Kv1	Kv2	Kv3	Kv4	Kv5	Kv6	Kv7	Kv8	Kv9	Kv10	Kv11	Kv12	Kv13	Kv14	Kv15	Kv16	Kv17
	2 DUN	1 DUN	1 PRD	1 PRX	1 MLT	2 MLT	2 Me-MLG	2 MLG	2 MLG	2 IJL	2 Ph	2 C I	2 C I	2 C I	2 C II	2 C III	2 C III
SiO <sub>2</sub>	37.42	38.67	36.98	41.02	42.21	41.76	39.36	45.45	45.19	44.34	28.78	0.96	1.96	3.26	0.95	0.42	1.09
TiO <sub>2</sub>	0.33	0.21	0.63	1.25	0.08	0.23	4.01	3.11	0.73	0.35	0.91	0.07	0.03	0.1	0.11	0.03	u.d.l.
Al <sub>2</sub> O <sub>3</sub>	0.74	0.79	1.22	5.75	4.14	7.98	13.18	10.42	8.52	23.54	9.45	0.38	0.14	0.36	0.19	0.07	0.31
Fe <sub>2</sub> O <sub>3</sub>	14.67	3.46	7.91	8.47	2.41	4.63	6.47	6.1	7.08	6.19	20.55	1.96	1.38	6.89	3.99	1.05	0.92
FeO	n.a.	10.21	7.58	5.31	2.88	n.a.	4.33	3.63	n.a.	n.a.	6.08	1.26	1.08	2.31	n.a.	1.53	–
MnO	0.33	0.48	0.41	0.15	0.06	0.09	0.15	0.17	0.23	0.06	0.24	0.07	0.08	0.12	0.07	0.19	0.18
MgO	45.75	44.33	37.65	17	10.79	9.3	6.99	6.06	8.05	2.03	26.37	1.61	3.01	5.35	1.87	19.81	20.62
CaO	0.57	1.09	3.55	14.33	34.61	30.2	15.56	14.04	19.12	5.97	3.73	51.7	51.57	45.03	49.7	31.05	30.96
Na <sub>2</sub> O	0.03	0.06	0.11	0.57	1.66	3.91	6.42	7.34	6.3	12.68	0.77	–	0.02	0.03	0.02	0.00	0.04
K <sub>2</sub> O	0.17	0.06	0.54	3.06	0.02	0.74	2.26	1.89	0.89	3.49	5.15	0.2	0.08	0.08	0.18	0.05	0.19
P <sub>2</sub> O <sub>5</sub>	0.01	0.03	0.03	0.23	0.04	–	0.3	0.67	2.24	0.63	2.36	0.33	0.89	0.1	1.9	1.53	1.08
LOI	–	0.43	2.06	1.44	0.1	1.41	0.43	0.72	1.55	0.56	0.95				37.49		
CO <sub>2</sub>												41.89	40.12	36.77		44.67	45.13
Total	100.02	99.64	98.67	98.58	98.99	100.25	99.46	99.55	99.9	99.84	98.31	100.43	100.36	100.40	96.47	100.40	100.52
Mg#	86.1	85.6	82.0	70.2	79.2	79.89	55.1	54.1	69.3	39.4	71.8						
A.I.	0.32	0.21	0.62	0.70	0.66	0.9	0.99	1.43	1.3	1.0	0.72						
Rb		9.7	11	103	1.1	24.1	37.1	26.8		29.8	144	5.88	4.9	3.13	14.3	6.6	10.4
Ba		157	269	1632	34	537	12.1	35.4		98	4895	317	246	208	531	46	72
Th		1.11	0.88	3.4	0.03	0.43	19.7	18		0.21	1.46	0.46	0.86	0.05	5.02	1.2	5.01
U		< 0.1	< 0.1	0.53		0.06	3.8	2.08		0.09	0.13	< 0.1	< 0.1	< 0.1	30.4	5.07	38.6
Nb		5.08	12.9	62	0.26	6.4	248	1312		24	61	5.21	2.56	6.86	76	31	84
Ta		0.47	1.22	2.2		0.27	7.23	33.6		3.5	9.9	0.75	0.47	2.11	27.6	6.42	35.2
Pb		< 0.5	< 0.5	1.63		4.3	6.3	0.68		1.74	2.2	0.99	< 0.5	< 0.5	< 0.5	< 0.5	< 0.5
Sr		59	87	293	2348	3798		306		595	186	3115	3045	2406	7036	3221	2778
Zr		8.31	51	246	4.7	10.9	162	451		43	336	42.5	105	282	144	3.87	3.07
Hf		< 0.1	0.73	3.8	0.03	0.23	5.5	10.1		1.47	8.8	0.59	1.62	5.6	3.32	< 0.1	< 0.1
Y		0.8	1.75	2.7	2.6	3.2	36	19.4		5.5	3.5	22.86	22.6	15.3	29	5.35	3.9
Zr/Hf			69.9	64.7	157	47.4	29.4	44.6		29.2	38.2	72	64.8	50.4	43.4		
Nb/Ta		10.8	10.6	28.2		23.7	34.3	39		6.9	6.2	6.9	5.4	3.25	2.75	4.83	2.4
Th/U				6.4		7.2	5.2	8.6		2.33	11.2				0.17	0.24	0.13

Table 4

REE data (in ppm) of the Kovdor silicate rocks and carbonatites

n.a.: not analyzed.

Normalizing values for  $(La/Yb)_N$  from Sun and McDonough (1989).

Sample Identification	Kv2 DUN	Kv3 PRD	Kv4 PRX	Kv5 MLT	Kv6 MLT	Kv7 Me-MLG	Kv8 MLG	Kv10 IJL	Kv11 Ph	AMD-WR Ph	AMD-Ap apatite-Ph	Kv12 C I	Kv13 C I	Kv14 C I	Kv15 C II	Kv16 C III	Kv17 C III
La	3.25	6.9	29	26	48	221	75	14.2	9.7	237	552	100	102	61	190	26.1	26.8
Ce	6.94	14.9	64	49	79	445	225	31	21	499	1185	183	190	114	467	56	56
Pr	0.43	1.52	6.9	5	8.3	48	31.2	3.9	2.8	n.a.	n.a.	20.5	21.6	12.9	39.7	6.3	6.42
Nd	1.19	5.46	23	17.4	27	161	116	15.1	11.2	300	716	72	76	45.7	140	22.6	22.9
Sm	0.11	0.72	3	2.1	3.2	21	17.1	2.3		39.9	98	10.2	10.7	6.53	18.5	3.2	3.05
Eu	0.04	0.22	0.78	0.59	0.81	6.5	4.4	0.64		11.6	27.3	2.89	3	1.9	4.97	0.91	0.83
Gd	0.29	0.71	1.94	1.65	2	18	9.69	1.68	1.55	29.6	69.7	7.57	7.92	5.11	12.6	2.48	2.11
Dy	0.11	0.38	0.86	0.65	0.86	10.8	5.79	0.9	0.86	15	43	4.7	4.89	3.23	6.94	1.3	1.01
Ho	0.02	0.07	0.1	0.08	0.09	1.73	0.9	0.11	0.11	n.a.	n.a.	0.91	0.87	0.62	1.15	0.23	0.16
Er	0.08	0.15	0.22	0.12	0.15	3.9	1.68	0.26	0.26	5.04	12.2	1.86	1.8	1.26	2.04	0.44	0.26
Yb	0.12	0.19	0.16	< 0.05	0.08	2.2	1.81	0.28	0.16	2.07	4.59	1.4	1.33	0.95	1.34	0.3	0.17
Lu	< 0.02	0.02	0.02	< 0.05	0.01	0.24	0.33	0.04	0.02	0.18	0.56	0.25	0.2	0.18	0.2	0.03	< 0.02
REE content	13	31	119	80	170	914	416	71	48	1144	2719	406	421	254	886	120	120
$(La/Yb)_N$	19	26	130		430	72	30	36	43	82	86	51	55	46	102	62	113

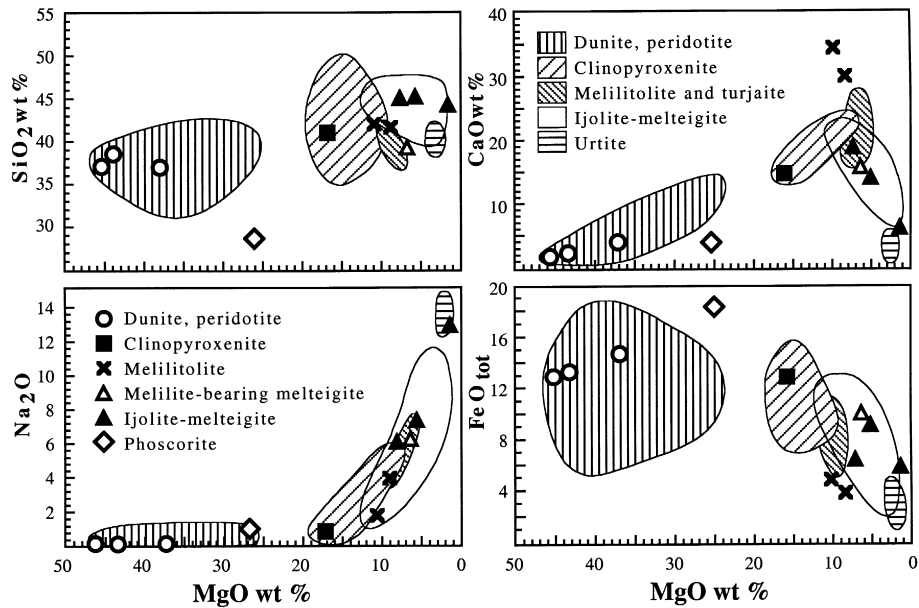


Fig. 3. Oxides (wt.%) vs. MgO (wt.%) diagram showing the compositional variations in the Kovdor whole rocks. The fields are from Arzamastsev (1994) data.

(grain size, mineralogy). Only the fine-grained phoscorite Kv11 has been analysed and may not be representative of the average phoscorite composition. It has a composition in the range of those of the ultramafic cumulates but with distinctly higher  $P_2O_5$  (2.3 wt.%),  $Al_2O_3$  (9.4 wt.%) and  $K_2O$  (5.1 wt.%) and lower  $SiO_2$  (28.5 wt.%) contents, reflecting the relatively high amounts of apatite and phlogopite in this sample. Apatite–magnetite ore rocks have extreme compositions, up to 30 wt.%  $FeO_{tot}$  and 22 wt.%  $P_2O_5$  (see analyses in Arzamastsev, 1994).

The carbonatites have generally less than 10 wt.%  $SiO_2$ . The first stage (C I) carbonatites plot in the calciocarbonatite field of the diagram of Woolley and Kempe (1989), except sample Kv14 that has a quite high modal content of olivine and magnetite. The  $SiO_2$  (< 3.6 wt.%) and MgO (1.6–5.4 wt.%) contents directly reflect the combined modal abundances of forsterite and phlogopite. The  $Al_2O_3$ ,  $K_2O$  and  $Na_2O$  contents are low, as in most plutonic carbonatites (Woolley and Kempe, 1989). The iron content is variable depending on the amount of magnetite (and of forsterite and phlogopite to a

lesser extent). Except CaO and MgO, most major elements are low in the dolomite carbonatites.

The trace elements abundance patterns, normalized to the primitive mantle values (Sun and McDonough, 1989) are presented in Fig. 4a–f for the ultramafic rocks, the ultramelilitolites, the ijolite–melteigite series, the phoscorite and the carbonatites. The elements are ordered, from left to right, by increasing compatibility in a mantle garnet lherzolite (Nelson et al., 1988). The ultramafic rocks show regular patterns with enrichment factors decreasing smoothly from the most to the least incompatible elements, i.e., in the dunite:  $Ba_N \sim 20$  to  $Zr_N \sim 0.8$ . There is an overall trace element enrichment in the sequence dunite–peridotite–clinopyroxenite. The patterns are characterized by a slight negative Rb anomaly and more pronounced Th (except the dunite) and U negative anomalies; HREE are largely depleted ( $Yb_N$  and  $Lu_N < 0.5$ ). Dunite shows a strong negative Hf anomaly. In contrast, the clinopyroxenite has a slight positive Zr–Hf anomaly which probably reflects the presence of perovskite. A positive Ta anomaly is observed in dunite and peridotite and in

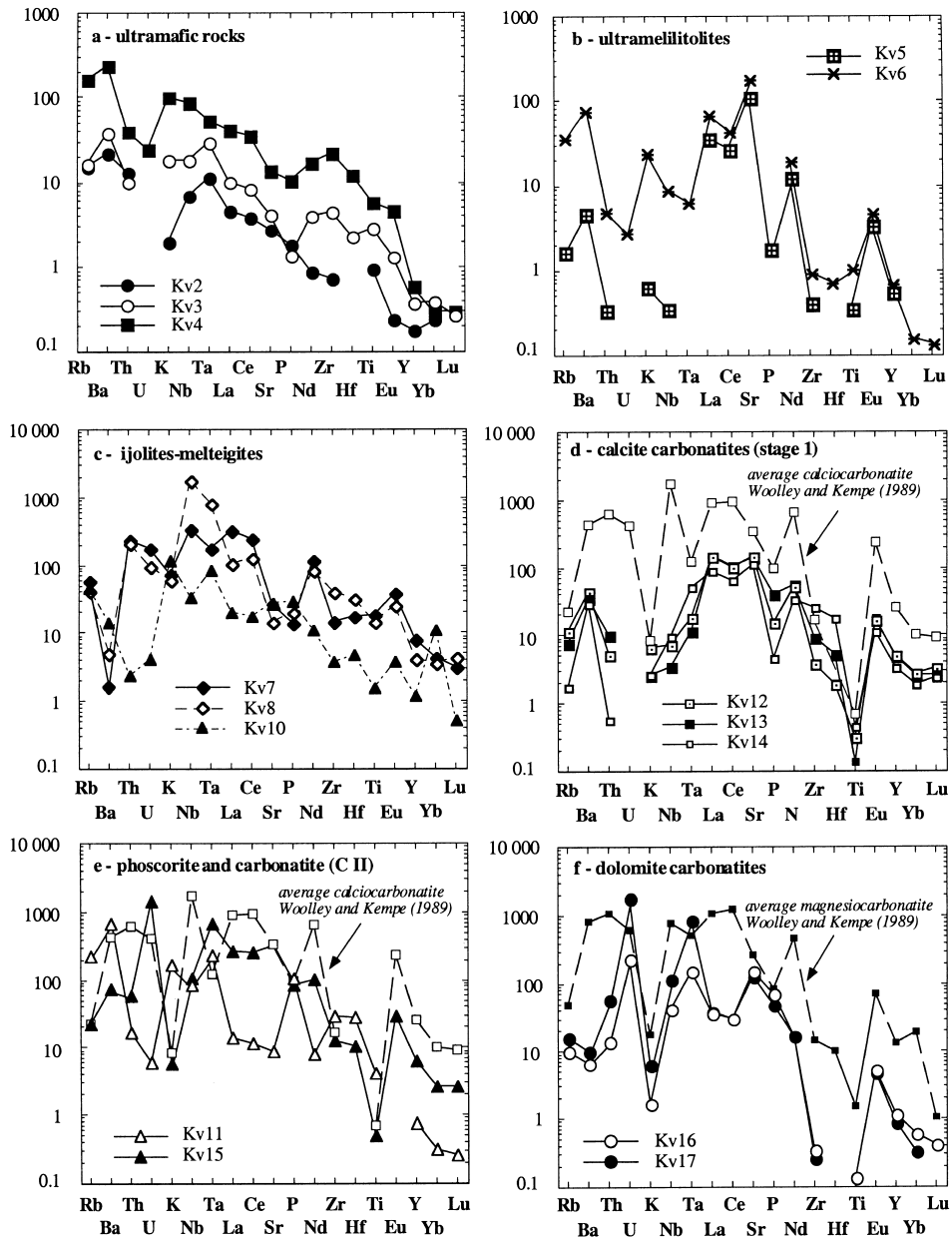


Fig. 4. Primitive mantle-normalized trace element abundances (normalizing values from Sun and McDonough, 1989). (a) Ultramafic rocks (dunite, peridotite and clinopyroxenite). (b) Ultramelilitolites. (c) Ijolites–melteigites. (d) Calcite carbonatites of the first stage (C I). (e) Calcite carbonatites of the second stage (C II) and phoscorites. (f) Dolomite carbonatites. Comparison with the average calcite carbonatite and dolomite carbonatite (Woolley and Kempe, 1989).

the carbonatites and phoscorites (see below). This anomaly does not seem to be related to any miner-

alogical control; it appears to reflect a geochemical feature of the parental magma. Similar Ta enrich-

ment was also observed in the ultramafic rocks of the Jacupiranga (Huang et al., 1995) and the Salitre (Morbidelli et al., 1997) complexes in Brazil.

The two analyzed ultramelilitolites have similar patterns. Most incompatible elements have low normalized abundances, often near or below 1. Some elements (Ba, Sr and L- to M-REE) are relatively enriched.

The ijolites–melteigites are, as a whole, enriched in all trace elements (enrichment factors higher than 1). The melteigites are particularly enriched in Th, U, Nb (positive anomaly), Ta and REE, reflecting the presence of perovskite and/of titanite. They

have large Ba, Sr and P negative anomalies and a less pronounced K anomaly. The ijolite (Kv10) is less enriched in incompatible elements than the melteigite, except in Ba and Sr; Th and U are severely depleted.

The phoscorite analyzed is strongly enriched in Ba, K, Ta, P, Zr and Hf. This composition is directly related to the liquidus phase assemblage (phlogopite and apatite) and to the accessory minerals (baddeleyite). Th, U, Ti and REEs have rather low normalized abundances.

The calcite carbonatites are characteristically enriched in Ba, Sr (up to 7550 ppm) and REE. Those

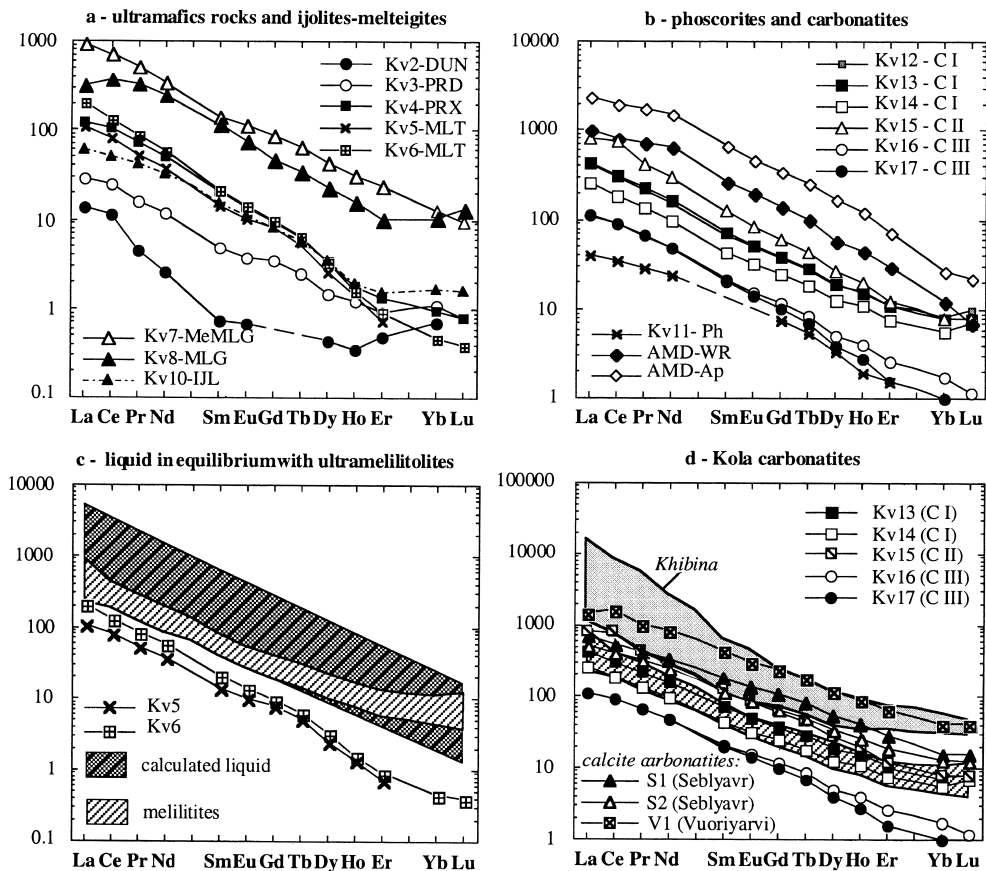


Fig. 5. Chondrite-normalized REE abundances (normalizing values from Sun and McDonough, 1989). (a) Ultramafic rocks, ultramelilitolites and ijolites–melteigites. (b) Calcite carbonatites of the first and second stages, dolomite carbonatites and phoscorites (WR: whole rock; Ap: apatite). (c) Measured ultramelilitolites and field of calculated liquids in equilibrium with these ultramelilitolites (see text for explanation). The simply hatched field corresponds to the Tersky Coast melilitites and kimberlites and the Kandalaksha ultramafic lamprophyres (Beard et al., 1996, 1998). (d) Comparison of the Kovdor carbonatites with other carbonatite occurrences from the Kola Peninsula (Khibina, Sebyavr, Vuoriyarvi; Verhulst et al., unpublished data; the simply hatched field, see c).

of the first stage show very deep negative U and Ti anomalies, a moderate negative P anomaly and positive Ba and Sr anomalies. In contrast, the calcite carbonatite of the second stage displays higher U, Th, Nb, Ta and REE content than those of the first stage. Dolomite carbonatites are strongly enriched in U and Ta; they have positive U, Ta and Sr anomalies and large negative Zr, Hf and Ti anomalies.

The chondrite-normalized REE abundances (Sun and McDonough, 1989) are shown in Fig. 5. All the rocks, either silicate or carbonatitic, are enriched in LREE with  $(La/Yb)_N$  ratios ranging from 19.5 to

130; the ultramelilitolites display extreme values, up to 430. The REE content increases more or less regularly through the silicate rock sequence but the ranges of the REE content ( $\Sigma REE$ ) for each group are partly overlapping: 12.6–130 ppm in the ultramafic cumulates, 103–170 ppm in the ultramelilitolites, 71 ppm for the ijolite up to 490–942 ppm in the melteigites. The patterns are relatively steep,  $(La/Yb)_N > 20$ , and roughly parallel, except for the dunite which has an upward concave pattern. This concave pattern is mainly due to a LREE enrichment that could be related to the presence of apatite (see

Table 5

Rb, Sr, Sm and Nd concentrations and Sr and Nd isotope composition of the Kovdor silicate rocks and carbonatites  
*i* means recalculated at 380 Ma.  
*m* for measured.

Samples	Rock type	Rb (ppm)	Sr (ppm)	$(^{87}\text{Sr}/^{86}\text{Sr})_m$	$2\sigma$	$(^{87}\text{Sr}/^{86}\text{Sr})_i$	
Kv1	DUN	2.6	18	0.706698	9	0.70444	
Kv2	DUN	9.7	59	0.707448	8	0.70487	
Kv3	PRD	11	87	0.705668	8	0.70369	
Kv4	PRX	102.7	293	0.709192	11	0.70370	
Kv5	MLT	1.1	2348	0.703490	10	0.70348	
Kv6	MLT	24.05	3798	0.704018	15	0.70392	
Kv7	Me-MLG	37.1	566	0.704799	10	0.70377	
Kv8	MLG	26.8	306	0.705750	13	0.70438	
Kv9	MLG	8.15	599	0.704793	11	0.70458	
Kv10	IJL	29.8	595	0.704481	13	0.70370	
Kv11	Ph	144	186	0.715668	16	0.70353	
AMD-WR	Ph	39	930	0.703980	90	0.70332	
AMD-Ap	Ph (apatite)	< 1	2001	0.703690	100	0.70368	
Kv13	C I	4.9	3045	0.703670	10	0.70364	
Kv16	C III	6.6	3221	0.703600	8	0.70357	
Kv17	C III	10.4	2778	0.703590	8	0.70353	
767/9	C I	< 1	4623	0.703460	40	0.70346	
9/85	C I	< 1	5208	0.703700	20	0.70370	
12009	C I	< 1	7069	0.703670	30	0.70367	
		Sm (ppm)	Nd (ppm)	$(^{143}\text{Nd}/^{144}\text{Nd})_m$	$2\sigma$	$(^{143}\text{Nd}/^{144}\text{Nd})_i$	$\epsilon_{\text{Nd}}(i)$
Kv2	DUN	0.11	1.19	0.512545	21	0.51241	+ 5.0
Kv3	PRD	0.72	5.46	0.512568	18	0.51237	+ 4.3
Kv4	PRX	3	23	0.512375	12	0.51218	+ 0.6
Kv5	MLT	2.1	17.4	0.512467	27	0.51228	+ 2.7
Kv6	MLT	3.2	27	0.512429	14	0.51225	+ 2.0
Kv7	Me-MLG	21	161	0.512522	13	0.51233	+ 3.4
Kv8	MLG	17.1	116	0.512426	8	0.51220	+ 1.1
Kv10	IJL	2.3	15.1	0.512204	10	0.51198	- 3.4
AMD-Ap	Ph (apatite)	98	716	0.512590	10	0.51238	+ 4.6
Kv13	C I	10.7	76	0.512441	9	0.51223	+ 1.6
767/9	C I	9.9	85	0.512590	10	0.51242	+ 5.2
12009	C I	12.6	123	0.512460	10	0.51231	+ 3.1
Kv16	C III	3.2	22.5	0.512484	21	0.51227	+ 2.4

discussion). Two rocks of the melteigite–ijolite series have flat HREE patterns; the third sample (Kv7) shows decreasing REE abundances with increasing atomic number. The presence of aegirine–augite instead of diopside could explain this difference (Bea, 1996). These alkaline silicate rocks do not show any Eu anomaly. The two phoscorites analyzed for REE have contrasting content (47.9–1143 ppm) but similar slopes: the REE content of sample AMD-WR seems to be controlled by apatite (AMD-Ap, Fig. 5b). In the calcite carbonatites, the LREE content increases from the first to the second stage while the HREE remain quite constant (Fig. 5b). Consequently, the  $(\text{La}/\text{Yb})_N$  ratio is significantly higher ( $\sim 100$ ) in the second stage than in the first (46–55). Dolomite carbonatites have lower REE content ( $\text{La}_N$ : 100) than calcite carbonatites ( $\text{La}_N$ : 200–800). This is the opposite to what is commonly observed in carbonatite intrusions elsewhere in the world (Woolley and Kempe, 1989) but a similar behavior has been observed in the Turij massif (Dunworth and Bell, submitted) and in the Lueshe massif (van Overbeke et al., 1996). Moreover, the REE contents of most Kovdor carbonatites are significantly lower than other calcite carbonatites of the Kola province (i.e., Khibina, Seblyavr, Vuoriyarvi and Ozernaya Varaka; Kramm and Kogarko, 1994; Verhulst et al., unpublished data, see Fig. 5d). This relatively low REE content in Kovdor carbonatites and its decrease from calcite carbonatites to dolomite carbonatites could result from the fractionation of apatite and other REE-rich accessory minerals in the phoscorites. Some phoscorites have up to 22 wt.%  $\text{P}_2\text{O}_5$ ; apatite separated from these rocks are REE-rich (2720 ppm; see sample AMD-Ap, Table 4).

### 5.2. Isotope compositions

The Sr and Nd isotopic data of carbonatites and related rocks from Kovdor are given in Table 5. As Kovdor is a multiphase intrusion, all the samples might not have exactly the same age or, alternatively, might not have strictly the same initial isotopic composition. It is interesting to note, however, that in the Rb–Sr isochron diagram, the silicate rocks (including the phoscorite Kv11) are roughly aligned along a reference line (it is in fact an errorchron with a MSWD value of 25) that gives an

age indication of  $370 \pm 8$  Ma ( $2\sigma$ ). This agrees, within error limits, with the baddeleyite U–Pb age of  $380 \pm 4$  Ma obtained by Bayanova et al. (1997). The initial isotopic ratios have been recalculated for each sample, assuming an age of 380 Ma. Most ultramafic and alkaline silicate rocks, including the melilite-bearing melteigite Kv7, have  $(^{87}\text{Sr}/^{86}\text{Sr})_i$  in a narrow range of values: 0.70369–0.70377. The two analyzed dunites have more radiogenic Sr isotope compositions, 0.70444 and 0.70487, respectively. The two ijolites–melteigites Kv8 and Kv9 also have distinctly higher initial ratios, 0.70441 and 0.70743, respectively.

The carbonatites (both calcite-bearing and dolomite-bearing varieties) and the phoscorite show a rather narrow range of  $(^{87}\text{Sr}/^{86}\text{Sr})_i$  from 0.70320 to 0.70370. Apatite (sample AMD-Ap) separated from the phoscorite AMD-WR has a slightly higher initial ratio (0.70368) than its whole rock (0.70332) but both values fall within the restricted range of values shown by the carbonatites and phoscorites. The two analysed ultramelilitolites also have Sr isotopic compositions (0.70348–0.70392) within the range of isotope data from the ultramafic cumulates and carbonatites.

The initial Nd isotopic compositions, expressed as  $\varepsilon_{\text{Nd}}(t)$ , have been calculated at 380 Ma. Except for the ijolite Kv10 that has a negative value ( $\varepsilon_{\text{Nd}}$ :  $-3.4$ ), all the rocks have positive  $\varepsilon_{\text{Nd}}(t)$  values. The measured ranges are, respectively:  $+0.6$  to  $+5.0$  for the ultramafic cumulates,  $+1.1$  to  $+3.5$  for the melteigite–ijolite series,  $+2.0$  to  $+2.7$  for the ultramelilitolites and  $+1.6$  to  $+5.2$  for the calcite-bearing and dolomite-bearing carbonatites. These ranges are largely overlapping. Moreover, it appears that the Nd isotopic composition varies more widely than the Sr isotopic composition.

## 6. Discussion

### 6.1. Crystallization history and nature of the parental magma(s) of the Kovdor massif

The ultramafic rocks (dunite, clinopyroxenite and melilitolite) have obvious cumulate textures, implying fractionation and accumulation of olivine,

clinopyroxene (diopside) and melilite. The order of crystallization can be deduced from the field relations and from petrographic observations. The following crystallization sequence is proposed: olivine is the earliest phase on the liquidus, followed by clinopyroxene, melilite, and finally nepheline. This observed sequence is in agreement with the experimental investigations of Onuma and Yamamoto (1976) on the system diopside–nepheline–åkermanite–silica.

Magnetite and phlogopite are ubiquitous interstitial phases in the ultramafic rocks and in the melilitolites. The status of these minerals has been debated: Kukharensko et al. (1965) suggested that they are late metasomatic phases but they can also be interpreted as intercumulus phases. In their recent detailed study of crystallized melt inclusions, Veksler et al. (1998a) have found both phlogopite and magnetite in the inclusions of the main minerals of all the Kovdor rocks. This important observation allows to deduce that phlogopite and magnetite were primary magmatic phases (on the liquidus) and not late metasomatic phases. Therefore, the variable modal abundances of these two minerals can directly be related to the amount of interstitial (= intercumulus) liquid. Variations in major and trace elements observed in the cumulates can then also be linked to the variable proportion of this trapped liquid.

The melilitolites and the associated turjaites on one hand, and the rocks of the melteigite–ijolite series on the other hand, are very heterogeneous, both in the field and in thin sections (Kukharensko et al., 1965; Arzamastsev, 1994, 1995; this study). The fractionation history for these rocks is not as clear as in the ultramafic cumulates. It nevertheless appears that melilite, nepheline, clinopyroxene (diopside to aegirine–augite) ± phlogopite all fractionate, leading to the formation of melilitolite, turjaite and melilite-bearing melteigite. The rocks of the melteigite–ijolite series (except the melilite-bearing melteigites) could correspond to a second, contaminated series (see below). A similar scenario has been proposed by Nielsen and Holm (1993) for the Gardiner complex of Greenland.

Chemical characteristics of the parental magma (or magmas, as several distinct batches are probably involved), as inferred from cumulus mineral chemistry and mineralogical associations, suggest high

MgO, CaO and low SiO<sub>2</sub> contents. The magmatic origin of phlogopite indicates a relatively water-rich melt. The presence of interstitial primary calcite (Verhulst et al., 1997) between the cumulus minerals in the ultramafic rocks and of calcite (and Na–Ca carbonate) in the crystallized melt inclusions (Veksler et al., 1998a) indicate CO<sub>2</sub>-bearing primary melt(s). Therefore, a mechanism involving fractional crystallization of several batches of a carbonated olivine melanephelinite parental magma can be inferred to have produced the various Kovdor rocks (Kukharensko et al., 1965; Veksler et al., 1998a).

However, despite large modal variations and evidence of fractionation, cryptic compositional variations of the main minerals (olivine and clinopyroxene) in the ultramafic sequence (dunite, peridotite and clinopyroxenite) have not been observed. This absence of cryptic variation, together with disequilibrium textures (tentatively attributed to magma mixing, *sensu* Rock et al., 1994) observed in the ijolite–melteigite series preclude a simple, progressive, differentiation trend by fractional crystallization in a closed-system.

The ultramafic cumulate rocks (dunite–clinopyroxenite sequence) are distinctly enriched in incompatible trace elements (i.e., the clinopyroxenite has LREE<sub>N</sub> values around 100) when compared to mantle-derived peridotite massifs and ultramafic xenoliths (i.e., McDonough and Frey, 1989). This enrichment could be due to their derivation from a parental magma strongly enriched in incompatible elements (very low degree of partial melting) or more probably to the presence of intercumulus material in the analyzed rocks. Moreover, there is a gradual increase of incompatible trace elements and REE content from dunite to clinopyroxenite. This can theoretically be interpreted as resulting either from a normal fractional crystallisation process, or from increasing proportions of trapped intercumulus liquid in the cumulates or from the derivation of the different cumulates from a series of increasingly enriched magma batches. As cryptic variations of the composition of the cumulus minerals (olivine and clinopyroxene) were not observed, the first hypothesis can be discarded. Although one cannot rule out the possibility that the minerals of the ultramafic cumulates were thoroughly reequilibrated during a late (sub-solidus) recrystallization, there are no convincing

field and petrographic arguments to support this hypothesis.

The level of emplacement is difficult to estimate. Taking into account the presence of diopside lamellae (probably formed by exsolution) in the olivines, the range of CaO content of the primary olivine is tentatively estimated at about 0.4–0.7 wt.% (maximum 2 vol.% of exsolutions and relative diopside:magnetite proportion of 3:1), which is slightly higher than in the olivine from the olivine melanephelinite from Turiy Mys (0.46–0.5 wt.%; Ivanikov et al., 1998). This quite high CaO content would indicate crystallization in a shallow magma chamber (Simkin and Smith, 1970). Epshteyn and Kaban’Kov (1984) have independently estimated the depth of emplacement of the Kovdor massif at  $4 \pm 0.7$  km from the homogenization temperature of fluid inclusions in quartz and apatite from late-stage ankeritic and dolomitic-quartz bearing carbonatite.

## 6.2. Genetic relations and characteristics of the mantle source(s)

The initial (at 380 Ma) isotopic compositions —  $(^{87}\text{Sr}/^{86}\text{Sr})_i$  and  $\varepsilon_{\text{Nd}}(t)$  — are plotted in the classi-

cal Nd–Sr diagram (Fig. 6). Published data from the literature for the Kola alkaline and carbonatitic province are added (Kramm, 1993; Kramm and Kogarko, 1994; Zaitsev and Bell, 1995; Beard et al., 1996, 1998; Demaiffe et al., 1997). The carbonatites, phoscorites, ultramafic cumulates (see discussion for the dunites, below), ultramelilitolites and melilite-bearing melteigite (Kv7) define a wide field in the depleted mantle (upper left) quadrant of the diagram. The range of  $\varepsilon_{\text{Nd}}(t)$  values (+5.2 to +0.6, corresponding to  $^{143}\text{Nd}/^{144}\text{Nd}$  ratios in the range 0.512179–0.512416) is significantly larger than the range of  $^{87}\text{Sr}/^{86}\text{Sr}$  ratios (0.70332–0.70377). Broadly speaking, these data show that all the rocks were derived from a source (or several sources) that had a time-integrated depletion in LIL elements (Rb and LREE). This source is not as severely depleted as the typical asthenospheric N-MORB source, it is more comparable to an OIB-type source (Nelson et al., 1988). In fact, our data for Kovdor, as well as most isotopic data for the other Kola carbonatites and related rocks, plot close to the “mantle array” recalculated at 380 Ma (Dostal et al., 1998). A plume (= deep mantle) component in the parental

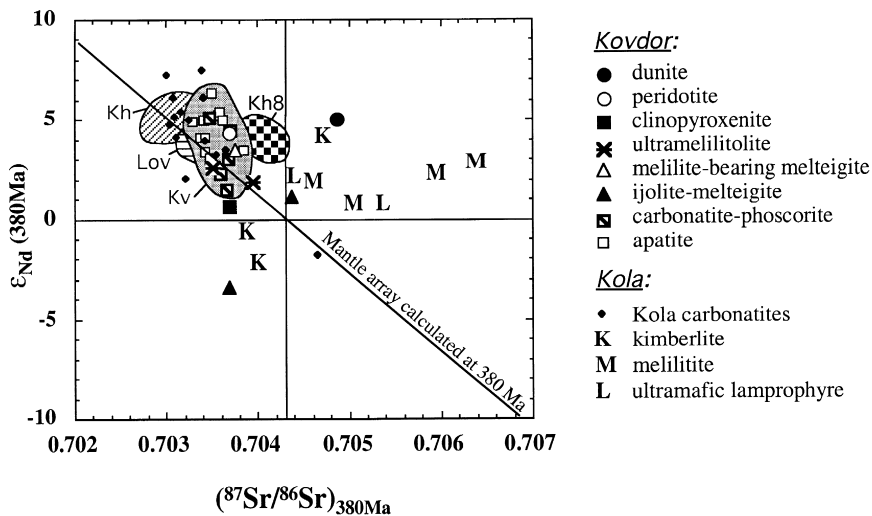


Fig. 6. Nd–Sr isotopic data for Kovdor rocks: apatite data of Zaitsev and Bell (1995). Comparison with other rocks from the Kola Peninsula: the Kola carbonatites (Sebyavr, Vuoriyarvi, Sokli, Ozernaya Varaka, Turiy Mys and Telyachi Island) from Kramm (1993), Verhulst et al. (unpublished data) and Beard et al. (1996); the kimberlites (K), melilitites (M) and ultramafic lamprophyres (L) of the Kandalaksha Gulf and the Tersky Coast from Beard et al. (1996; 1998); fields for the Khibina (Kh) and Lovozero (Lov) nepheline syenites and the Khibina carbonatites (Kh8) are deduced from the data of Kramm and Kogarko (1994). Mantle array recalculated at 380 Ma (Dostal et al., 1998).

magma(s) of the Kola ultramafic alkaline province is also indicated by noble gas concentrations and isotopic compositions. Quite high  $^3\text{He}$  abundances ( $5 \times 10^{-9}$  to  $5 \times 10^{-10}$   $\text{cm}^3$  STP  $\text{g}^{-1}$ ) and low  $^4\text{He}/^3\text{He}$  isotopic ratios ( $3 \times 10^4$  to  $10^5$ ) (comparable to or lower than the MORB value:  $8.9 \times 10^4$ ; Toltstikhin and Marty, 1999) have been measured for ultramafic rocks and carbonatites of Kovdor and Seblyavr (another intrusion of the same province) (Marty et al., 1998; Toltstikhin et al., 1998). So the mantle signature is preserved and crustal influence is not detectable in the Sr and Nd isotopic data. This is not surprising in view of the very high Sr (up to 7100 ppm) and LREE (up to 720 ppm Nd) contents of most of these rocks. In detail, however, Kovdor carbonatites and phoscorites show a wide range of initial  $^{87}\text{Sr}/^{86}\text{Sr}$  ratios and  $\varepsilon_{\text{Nd}}(t)$  values. Our data on whole rock calcite carbonatites and dolomite carbonatites plot between the two groups of carbonatites and phoscorites defined by Zaitsev and Bell (1995) on the basis of the Sr–Nd isotopic compositions of apatite. We do not observe any obvious relation between the isotopic compositions and the Sr and Nd contents of our whole-rock data, as tentatively suggested by Zaitsev and Bell (1995). As crustal contamination appears unlikely, this large range of isotopic composition is probably best explained by mixing processes involving either several melt batches formed in an isotopically heterogeneous source or various mixing proportions of two isotopically distinct sources. Such open system behavior has already been proposed for other carbonatitic intrusions (Jacupiranga, Brazil; Huang et al., 1995).

In his first paper on the isotopic composition of the Kola carbonatites, Kramm (1993) suggested that his data define a line — the Kola carbonatite line (KCL) — extending from the depleted quadrant to the enriched field. In fact, the “enriched end” of this line was based on only one sample, a carbonatite from the Vuoriyarvi intrusion ( $\varepsilon_{\text{Nd}} = -1.94$  and  $(^{87}\text{Sr}/^{86}\text{Sr})_i = 0.70466$ ). We have analyzed another carbonatite from this massif (sample Ko349-78): it plots in the depleted quadrant with  $\varepsilon_{\text{Nd}} = +4.6$  and  $(^{87}\text{Sr}/^{86}\text{Sr})_i = 0.70306$ . The carbonatite analyzed by Kramm could have been contaminated by crustal material as modal quartz was observed (Kramm, personal communication). It does appear, from our data and from the data compilation, that the Kola

carbonatites define a broad field in the depleted mantle quadrant rather than a well-defined line.

The ultramelilitolites have isotopic compositions that plot in the main Kovdor domain, implying their derivation from the same source (or sources) as the carbonatites and the ultramafic cumulates. These data thus confirm the magmatic origin of the melilitolite as already suggested by the melilite chemical composition and by the high (970–1080°C) homogenization temperatures of the melt inclusions in melilite from a turjaite (Veksler et al., 1998a).

A few Kovdor rocks have isotopic compositions that plot outside the depleted quadrant of the Nd–Sr diagram.

(1) The analyzed dunite plots in the upper right quadrant: while its Nd isotopic signature is comparable to those of the other ultramafic cumulates, its Sr isotopic composition is shifted to significantly higher values (0.70487). This dunite has the lowest Sr (18–59 ppm) and Nd (< 2 ppm) contents and hence it could have been easily contaminated by the surrounding Archean gneisses. However, this crustal contamination process should also have shifted the Nd isotopic composition to negative  $\varepsilon_{\text{Nd}}(t)$  values. Unfortunately, isotopic data on the gneisses surrounding the Kovdor massif are lacking so that this contamination hypothesis cannot be further tested.

(2) The melteigite–ijolite series is isotopically very heterogeneous;  $(^{87}\text{Sr}/^{86}\text{Sr})_i$  vary from 0.70370 to 0.70458 and  $\varepsilon_{\text{Nd}}(t)$  from +3.5 to –3.6. There is no relation between the Nd and Sr isotopic compositions. The melilite-bearing melteigite Kv7 plots in the field of most Kovdor rocks, in the depleted mantle quadrant. The melteigite with the highest initial  $^{87}\text{Sr}/^{86}\text{Sr}$  ratio (Kv8) still has a positive  $\varepsilon_{\text{Nd}}$  while the ijolite with negative  $\varepsilon_{\text{Nd}}(t)$  value (Kv10) has a low  $^{87}\text{Sr}/^{86}\text{Sr}$  ratio. Interestingly, these isotopic heterogeneities are observed for the melteigites that also show local petrographic heterogeneities (Kukharenko et al., 1965; Arzamastsev, 1994) and textural disequilibrium in thin sections. Indeed, the clinopyroxene of sample Kv9 shows core resorption and highly complex zoning; the perovskite and the aegirine–augite are replaced by titanite in sample Kv8. These features could indicate that the melteigite melt evolved under open-system conditions, maybe involving magma mixing (Rock et al., 1994). In that hypothesis, the melteigite melt would have mixed

with a melt displaying slightly enriched isotopic characteristics as shown by the Kandalaksha ultramafic lamprophyres and melilitites and by the Tersky Coast and Arkhangelsk kimberlites (Beard et al., 1996, 1998, this volume). Alternatively, the position of the ijolite in the lower left quadrant of the Nd–Sr diagram could be explained by contamination with lower crustal granulites as suggested, for example, by the Sr–Nd and Pb isotopic composition for the Oldoinyo Lengai ijolites (Bell and Simonetti, 1996) and for the Shombole (E. Africa) phonolites (Bell, 1998). Our data on the Kovdor melteigites–ijolites are not in favour of the origin of the ijolite by rheomorphism of fenitized wall rocks as suggested by Kramm (1994) for the ijolite of the type locality (Iivaara).

### 6.3. Magmatic processes: liquid immiscibility vs. fractional crystallization

Liquid immiscibility has long been recognized (i.e., Le Bas, 1977) as a possible process to generate carbonatite liquid and a conjugate silicate liquid of phonolitic (= ijolitic) composition. The two conjugate immiscible liquids must necessarily have the same Sr and Nd isotopic compositions. This is obviously not the case for the Kovdor carbonatites and ijolite–melteigite series rocks. (This difference could be explained by an AFC process as it is probable that assimilation would affect the silicate liquid more easily than the carbonatite liquid; see Ray, 1998.) Moreover, available trace element (Nb, Ta and REE) data show that the calculated partition coefficients for the Kovdor carbonatite and silicate rocks ( $D^{\text{carb-silic}}$ ) are not in agreement with the recent experimental values (Veksler et al., 1998b) for carbonatite–silicate immiscible pairs. A recent study of the crystallized melt inclusions in the main minerals from Kovdor (Veksler et al., 1998a) has also concluded that the carbonatites more probably result from a simple fractional crystallization process.

Disequilibrium textures observed in ijolites–melteigites and the poorly known partition coefficients of many trace elements (including the REE) for the carbonate minerals and for many accessory minerals preclude modelling of the liquid's composition in equilibrium with most rocks. The approach can nevertheless be applied to ultramelilitolites which

are melilite cumulates (> 85 vol.%). Using the solid/silicate liquid trace elements partition coefficients for melilite (Nagasawa et al., 1980; Kuehner et al., 1989), the composition of the liquid in equilibrium can be calculated: it is extremely enriched in Sr (2134–6125 ppm) and LREE (52–571 ppm La) and depleted in M- to HREE (0.1–0.4 ppm Yb). The REE pattern of the calculated liquid in equilibrium with the ultramelilitolites (Fig. 5c) is quite similar to the patterns of the Kovdor carbonatites. Interestingly, the REE pattern of this calculated liquid is also fairly comparable to those of the melilitites and ultramafic lamprophyres of the nearby Kandalaksha dyke system and Tersky Bereg domain (Beard et al., 1996, 1998) that represent magmatic liquids (not cumulates) intruded penecontemporaneously with the Kovdor (and the other) ultramafic and carbonatite complexes.

## 7. Conclusions

Petrographical, geochemical (major and trace elements) and Sr–Nd isotopic data have been obtained for the various lithological units that compose the Kovdor ultramafic, alkaline and carbonatite intrusion. The main conclusions are summarised below.

(1) The dunites–clinopyroxenites and the melilitolites are cumulates, implying olivine + diopside + melilite  $\pm$  nepheline fractionation from several high-Mg, high-Ca parental magma pulses of olivine melanephelinite composition.

(2) The carbonatites (and their associated phosphorites) and the differentiated alkaline silicate rocks (ijolite–melteigite series) are not conjugate immiscible liquids. Carbonatites and melilitolites appear to be derived from a common Sr- and LREE-rich liquid comparable to the Kandalaksha melilitites and lamprophyres.

(3) Initial isotopic data of the ultramafic cumulates, the melilitolites and the carbonatites plot close to the mantle array at 380 Ma, in the depleted quadrant of the Nd–Sr diagram. The dispersion of data suggests either that several magma batches were derived from an isotopically heterogeneous mantle source or that two mantle components (a depleted mantle and a plume type component) were mixed in various proportions.

(4) The rocks of the melteigite–ijolite series are heterogeneous and show disequilibrium textures. Their isotopic composition (positive and negative  $\varepsilon_{\text{Nd}}$  values) requires an enriched component that could correspond to the source of the contemporaneous ultramafic lamprophyres and the Arkhangelsk kimberlites.

## Acknowledgements

This work has been supported by an INTAS grant (project No. 94-2621) to D.D. Dr. I. Tolstikhin (Apatity, Russia) initiated the collaboration between the Belgian and the Russian teams. Prof. F. Mitrofanov (Kola Center, Apatity, Russia) allowed us to study the Kola alkaline province. Drs. V. Vetrin and V. Nivin are warmly thanked for the perfect organization of the field trips. The paper has been greatly improved by the constructive comments and suggestions of Dr. T. Nielsen and Dr. E. Dunworth. Participants involved in the EUROPROBE–SVEKA–LAPKO project are thanked for discussion during the Lammi (Finland) and Repino (Russia) meetings. We thank Dr. D. Weis (Univ. Brussels) for her assistance during the isotope measurements and N. Cromps for the drawing of the figures. The mass spectrometric measurements in Brussels are supported by FNRS-FRFC grants to D.D.

## References

- André, L., Ashchepkov, I.V., 1996. Acid leaching experiments on the mantle-derived Vitim clinopyroxenes: implications for the role of clinopyroxenes in the mantle processes. In: Demaiffe, D. (Ed.), *Petrology and Geochemistry of Magmatic Suites of Rocks in the Continental and Oceanic Crusts*. ULB-MRAC, Brussels, pp. 321–336.
- Arzamastsev, A.A., 1994. Unique paleozoic intrusions of the Kola Peninsula. Geological Institute of the Kola Science Centre, Apatity, 79 pp.
- Arzamastsev, A.A., 1995. Paleozoic plutonic complexes. In: Mitrofanov, F.P. (Ed.), *Geology of the Kola Peninsula*. Apatity, pp. 85–103.
- Arzamastsev, A.A., Glasnev, V.N., Raevskii, A.B., 1996. The deep structure of carbonatite complexes in the Kola region: geological and geophysical data. *Trans. (Doklady) Russian Acad. Sci./Earth Sci. Sections* 348 (4), 578–580.
- Balaganskaya, E.G., 1994. Breccias of the Kovdor phoscorite–carbonatite deposit of magnetite and their geological meaning. *Zap. Vses. Mineral. Obshchest.* 2, 21–36, (in Russian).
- Bayanova, T.B., Kimarski, Yu.M., Levkovich, N.V., 1997. A U–Pb study of baddeleyite from rocks of the Kovdor massif. *Doklady Akademii Nauk* 356, 509–511, (in Russian).
- Bea, F., 1996. Residence of REE, Y, Th and U in granite and crustal protoliths; implications for the chemistry of crustal melts. *J. Petrol.* 37, 521–552.
- Beard, A.D., Downes, H., Hegner, E., Sablukov, S.M., Vetrin, V., Balogh, K., 1998. Mineralogy and geochemistry of Devonian ultramafic minor intrusions of the southern Kola Peninsula, Russia: implications for the petrogenesis of kimberlites and melilitites. *Contrib. Mineral. Petrol.* 130, 288–303.
- Beard, A.D., Downes, H., Vetrin, V., Kempton, P.D., Maluski, H., 1996. Petrogenesis of Devonian lamprophyre and carbonatite minor intrusions, Kandalaksha Gulf (Kola Peninsula, Russia). *Lithos* 39, 93–119.
- Bell, K. (Ed.), 1989. *Carbonatites, Genesis and Evolution*. Unwin Hyman, London, 618 pp.
- Bell, K., 1998. Radiogenic isotope constraints on relationship between carbonatites and associated silicate rocks — a brief review. *J. Petrol.* 39 (11–12), 1987–1996.
- Bell, K., Blenkinsop, J., 1987a. Nd and Sr isotopic compositions of East African carbonatites: implications for mantle heterogeneity. *Geology* 15, 99–102.
- Bell, K., Blenkinsop, J., 1987b. Archean depleted mantle — evidence from Nd and Sr initial isotopic ratios of carbonatites. *Geochim. Cosmochim. Acta* 51, 291–298.
- Bell, K., Dunworth, E.A., Bulakh, A.G., Ivanikov, V.V., 1996. Alkalic rocks of the Turiy Massif, Kola Peninsula, including type-locality turjaite and turjite: a review. *Can. Mineral.* 34, 265–280.
- Bell, K., Simonetti, A., 1996. Carbonatite magmatism and plume activity: implications from the Nd, Pb and Sr isotope systematics of Oldoinyo Lengai. *J. Petrol.* 137, 1321–1339.
- Bykova, A.V., Iljinsky, G.A., 1978. Evolution of magnetite chemistry in rocks of Kovdor massif (Kola Peninsula). *Zap. Vses. Mineral. Obshchest.* 1, 21–32, (in Russian).
- Demaiffe, D., Verhulst, A., Weis, D., André, L., Nivin, V., 1997. Geochemical (major and trace elements) and Nd–Sr isotopic study of the Kovdor carbonatites (and related rocks) from the Kola Peninsula. *GAC/MAC Ann. Meeting (Ottawa)*, Abstr., p. 37.
- Dostal, J., Cousens, B., Dupuy, C., 1998. The incompatible element characteristics of an ancient subducted sedimentary component in ocean island basalts from French Polynesia. *J. Petrol.* 39, 937–952.
- Dudkin, O.B., Mitrofanov, F.P., 1994. Features of the Kola Alkali Province. *Geochem. Int.* 31 (3), 1–11.
- Dunworth, E.A., Bell, K., 1998. Melilitolites: a new scheme of classification. *Can. Mineral.* 36, 895–903.
- Dunworth, E.A., Bell, K., submitted. Isotopic and geochemical disequilibrium — evidence for multi-source evolution of the Turiy Massif, Kola Peninsula, Russia. *J. Petrol.*
- Epshteyn, Ye.M., Kaban’Kov, Ya.V., 1984. The depth of emplacement and mineral potential of ultramafic, ijolite and carbonatite plutons. *Int. Geol. Rev.* 26, 1402–1415.
- Gee, D.G., Zeyen, H.J. (Eds.), 1996. *EUROPROBE 1996 — lithosphere dynamics: origin and evolution of continents*. EUROPROBE, Uppsala University, 138 pp.

- Harker, R.I., Tuttle, O.F., 1956. The lower limit of stability of åkermanite ( $\text{Ca}_2\text{MgSi}_2\text{O}_7$ ). *Am. J. Sci.* 254, 468 and 478.
- Heinrich, E.W., 1966. *The Geology of Carbonatites*. Rand McNally, Chicago, 555 pp.
- Huang, Y.M., Hawkesworth, C.J., van Calsteren, P., McDermott, F., 1995. Geochemical characteristics and origin of the Jacupiranga carbonatites, Brazil. *Chem. Geol.* 119, 79–99.
- Ivanikov, V.V., Rukhlov, A.S., Bell, K., 1998. Magmatic evolution of the melilitite–carbonatite–nephelinite dyke series of the Turiy Peninsula (Kandalaksha Bay, White Sea, Russia). *J. Petrol.* 39 (11–12), 2043–2059.
- Kogarko, L.N., 1987. Alkaline rocks of the eastern part of the Baltic Shield (Kola Peninsula). In: Fitton, J.G., Upton, B.G.J. (Eds.), *Alkaline Igneous Rocks*, Vol. 30. The Geological Society Spec. Publ., pp. 531–544.
- Kogarko, L.N., Kononova, V.A., Orlova, M.P., Woolley, A.R., 1995. *Alkaline Rocks and Carbonatites of the World: Part 2. Former USSR*. Chapman and Hall, London, 225 pp.
- Kramm, U., 1993. Mantle components of carbonatites from the Kola Alkaline Province, Russia and Finland: a Nd–Sr study. *Eur. J. Mineral.* 5, 985–989.
- Kramm, U., 1994. Isotope evidence for ijolite formation by fenitization: Sr–Nd data of ijolites from the type locality Iivaaara, Finland. *Contrib. Mineral. Petrol.* 115, 279–286.
- Kramm, U., Kogarko, L.N., 1994. Nd and Sr isotope signatures of the Khibina and Lovozero agpaitic centres, Kola Alkaline Province, Russia. *Lithos* 32, 225–242.
- Kramm, U., Kogarko, L.N., Kononova, V.A., Vartiainen, H., 1993. The Kola Alkaline Province of the CIS and Finland: precise Rb–Sr ages define 380–360 Ma age range for all magmatism. *Lithos* 30, 33–44.
- Krasnova, N.I., Kopylova, L.N., 1988. The geologic basis for mineral–technological mapping at the Kovdor ore deposit. *Int. Geol. Rev.* 30, 307–319.
- Kratz, K.O., Glebovitskiy, R.V., Bilinskiy, V.L., Duk, I.B., Litvinenko, E.V., Sharkov, G.A., Porotova, S.A., Ankudinov, L.N., Platonenkova, L.N., Kokorina, L.K., Lazarev, Y.K., Platonova, A.P., Koshekin, B.I., Lvukashev, A.D., Stelkov, S.A., 1978. The earth's crust in the eastern part of the Baltic Shield, Nauka, Leningrad, 232 pp. (in Russian).
- Kuehner, S.M., Laughlin, J.R., Grossman, L., Johnson, M.L., Burnett, D.S., 1989. Determination of trace element mineral/liquid partition coefficients in melilite and diopside by ion and electron microprobe techniques. *Geochim. Cosmochim. Acta* 53, 3115–3130.
- Kukhareenko, A.A., Orlova, M.P., Boulakh, A.G., Bagdasarov, E.A., Rinskaya-Korsakova, O.M., Nefedov, E.I., Ilinskiy, G.A., Sergeev, A.S., Abakumova, N.B., 1965. The Caledonian complex of ultrabasic alkaline rocks of the Kola Peninsula and north Karelia. Nedra, Moscow, 772 pp. (in Russian).
- Larsen, L.M., Rex, D.C., 1992. A review of the 2500 Ma span of alkaline–ultramafic, potassic and carbonatitic magmatism in West Greenland. *Lithos* 28, 367–402.
- Le Bas, M.J., 1977. *Carbonatite–Nephelinite Volcanism*. Wiley, London, 347 pp.
- Le Maitre, R.W. (Ed.), 1989. *A Classification of Igneous Rocks and Glossary of Terms*. Blackwell, Oxford, 129 pp.
- Marty, B., Tolstikhin, I., Kamensky, I.L., Nivin, V., Balagan-skaya, E., Zimmermann, J.L., 1998. Plume-derived rare gases in 380 Ma carbonatites from the Kola region (Russia) and the argon isotopic composition of the deep mantle. *Earth Planet. Sci. Lett.* 164, 179–192.
- McDonough, W.F., Frey, F.A., 1989. Rare earth elements in upper mantle rocks. In: Lipin, B.R., McKay, G.A. (Eds.), *Geochemistry and Mineralogy of Rare Earth Elements*. *Rev. Mineral.* 21, 99–145.
- McKenzie, W.S., Donaldson, C.H., Guilford, C., 1987. *Atlas of Igneous Rocks and their Textures*. Longman Scientific and Technical, London, 148 pp.
- Mitchell, R.H., 1996. The Melilitite clan. In: Mitchell, R.H. (Ed.), *Undersaturated Alkaline Rocks: Mineralogy, Petrogenesis and Economic Potential*. Mineral. Assoc. Canada, Short Course 24, 123–152.
- Mitrofanov, F.P. (Ed.), 1995. *Geology of the Kola Peninsula*. Apatity, 145 pp.
- Morbideilli, L., Gomes, C.B., Beccaluva, L., Brotzu, P., Conte, A.M., Ruberti, E., Traversa, G., 1995. Mineralogical, petrological and geochemical aspects of alkaline and alkaline–carbonatite association from Brazil. *Earth Sci. Rev.* 39, 135–168.
- Morbideilli, L., Gomes, C.B., Beccaluva, L., Brotzu, P., Garbarino, C., Riffel, B.F., Ruberti, E., Traversa, G., 1997. Parental magma characterization of Salitre cumulate rocks (Alto Paranaíba Alkaline Province, Brazil) as inferred from mineralogical, petrographic and geochemical data. *Int. Geol. Rev.* 39, 723–743.
- Moseley, D., 1984. Symplectic exsolution in olivine. *Am. Mineral.* 69, 139–153.
- Nagasawa, H., Schreiber, H.D., Morris, R.V., 1980. Experimental mineral/liquid partition coefficients of the rare earth elements (REE), Sc and Sr for perovskite, spinel and melilite. *Earth Planet. Sci. Lett.* 46, 431–437.
- Navez, J., 1995. Détermination d'éléments en traces dans les roches silicatées par ICP-MS. *Dept. Géol. MRAC, Rapp. Ann.* 93, 139–147.
- Nelson, D.R., Chivas, A.R., Chappell, B.W., McCulloch, M.T., 1988. Geochemical and isotopic systematics in carbonatites and implications for the evolution of ocean–island sources. *Geochim. Cosmochim. Acta* 52, 1–17.
- Nielsen, T.F., 1980. The petrology of a melilitolite, melteigite, carbonatite and syenite ring dyke system, in the Gardiner complex, East Greenland. *Lithos* 13, 181–197.
- Nielsen, T.F.D., Holm, P.M., 1993. Nd and Sr isotope compositions from the Gardiner complex, East Greenland Tertiary igneous province. *Bull. Geol. Soc. Denmark* 40, 280–287.
- Onuma, K., Yamamoto, M., 1976. Crystallization in the silica-undersaturated portion of the system diopside–nepheline–åkermanite–silica and its bearing on the formation of melilitites and nephelinites. *J. Fac. Sci. Hokkaido Univ.* 4 (17), 347–355.
- Platt, R.G., 1996. The ijolite-series rocks. In: Mitchell, R.H. (Ed.), *Undersaturated Alkaline Rocks: Mineralogy, Petrogenesis and Economic Potential*. Mineral. Assoc. Canada, Short Course 24, 101–122.

- Pouchou, J.L., Pichoir, F., 1991. Quantitative analysis of homogeneous or stratified microvolumes applying the model "PAP". In: Heinrich, K.F.J., Newbury, D.E. (Eds.), *Electron Probe Quantification*. Plenum, New York, pp. 31–75.
- Ray, J.S., 1998. Trace element and isotope evolution during concurrent assimilation, fractional crystallization, and liquid immiscibility of a carbonated silicate magma. *Geochim. Cosmochim. Acta* 62, 3301–3306.
- Rock, N.M.S., Gwalani, L.G., Griffin, B.J., 1994. Alkaline rocks and carbonatites of Amba Dongar and adjacent areas, Deccan Alkaline Province, Gujarat, India: 2. Complexly zoned clinopyroxene phenocrysts. *Mineral. Petrol.* 51, 113–135.
- Russel, H.D., Hiemstra, S.A., Groeneveld, D., 1954. The mineralogy and petrology of the carbonatite at Loolekop, Eastern Transvaal. *Trans. Geol. Soc. S. Africa* 57, 197–208.
- Simkin, T., Smith, J.V., 1970. Minor element distribution in olivine. *J. Geol.* 78, 304–325.
- Sokolov, S.V., 1989. Melilitite rocks in massifs composed of ultramafites, alkali rocks, and carbonatites. *Geokhimiya* 12, 1683–1693.
- Steiger, R.H., Jäger, E., 1977. Subcommittee on geochronology: convention on the use of decay constants in geo- and cosmochronology. *Earth Planet. Sci. Lett.* 36, 359–362.
- Sun, S.S., McDonough, W.F., 1989. Chemical and isotopic systematics of oceanic basalts: implications for mantle composition and processes. In: Saunders, A.D., Norry, M.J. (Eds.), *Magmatism in the Ocean Basins*, Vol. 42. *Geol. Soc. Spec. Publ.*, pp. 313–345.
- Ternovoy, V.I., Afanasiev, B.V., Sulimov, B.I., 1969. Geology and prospecting of the Kovdor vermiculite–phlogopite deposit. Leningrad, Nedra, 288 pp. (in Russian).
- Toltstikhin, I.N., Kamensky, I.L., Nivin, V.A., Vetrin, V.R., Balaganskaya, E.G., Ikorsky, S.V., Gannibal, M.A., Kirnarsky, Yu.M., Marty, B., Weis, D., Verhulst, A., Demaiffe, D., 1998. Low mantle plume component in 370 Ma old Kola ultrabasic–alkaline–carbonatite complexes: evidences from rare gas isotopes and related trace elements. *Russ. J. Earth Sci.* 1 (2), (electronic paper; English translation, Feb. 1999).
- Toltstikhin, I.N., Marty, B., 1999. The evolution of terrestrial volatiles: a view from helium, neon, argon and nitrogen isotope modelling. *Chem. Geol.*, in press.
- van Overbeke, A.C., Demaiffe, D., Verkaeren, J., 1996. The syenite–carbonatite complex of Lueshe (N-E Zaire): petrography, geochemistry and Rb–Sr chronology. In: Demaiffe, D. (Ed.), *Petrology and Geochemistry of Magmatic Suites of Rocks in the Continental and Oceanic Crusts*. ULB-MRAC, Brussels, pp. 355–369.
- Veksler, I.V., Nielsen, T.F.D., Sokolov, S.V., 1998a. Mineralogy of crystallized melt inclusions from Gardiner and Kovdor ultramafic alkaline complexes: implications for carbonatite genesis. *J. Petrol.* 39 (11–12), 2015–2031.
- Veksler, I.V., Petibon, C., Jenner, G.A., Dorfman, A.M., Dingwell, D.B., 1998b. Trace element partitioning in immiscible silicate–carbonate liquid systems: an initial experimental study using a centrifuge autoclave. *J. Petrol.* 39 (11–12), 2095–2104.
- Verhulst, A., Demaiffe, D., Ohnenstetter, D., Blanc, Ph., Balaganskaya, E., Kirnarsky, Yu., 1997. Cathodoluminescence petrography of carbonatites and associated alkaline silicate rocks from the Kola Peninsula (Russia). *GAC/MAC Ann. Meeting (Ottawa)*, Abstr., 152.
- Woolley, A.R., Bergman, S.C., Edgar, A.D., Le Bas, M.J., Mitchell, R.H., Rock, N.M.S., Scott Smith, B.H., 1996. Classification of lamprophyres, lamproites, kimberlites, and the kalsilitic, melilitic, and leucitic rocks. *Can. Mineral.* 34, 173–174.
- Woolley, A.R., Kempe, D.R.C., 1989. Carbonatites: nomenclature, average chemical compositions and element distribution. In: Bell, K. (Ed.), *Carbonatites: Genesis and Evolution*. Unwin Hyman, London, pp. 1–14.
- Zaitsev, A., Bell, K., 1995. Sr and Nd isotope data of apatite, calcite and dolomite as indicators of source and the relationships of phoscorites and carbonatites from the Kovdor massif, Kola Peninsula, Russia. *Contrib. Mineral. Petrol.* 121, 324–335.